2015

UNDERSTANDING THE FUNCTION OF DYRK1A THROUGH CHARACTERIZATION OF ITS INTERACTING PROTEINS

Varsha Ananthapadmanabhan
Virginia Commonwealth University

UNDERSTANDING THE FUNCTION OF DYRK1A THROUGH CHARACTERIZATION OF ITS INTERACTING PROTEINS

A thesis submitted in partial fulfillment of the requirements of the degree of Master of Science at Virginia Commonwealth University.

By

Varsha Ananthapadmanabhan
B. Tech., D.Y Patil University, Navi Mumbai

Thesis Director: Larisa Litovchick, M.D., Ph.D.
Assistant Professor
Division of Hematology/Oncology and Palliative Care
Department of Internal Medicine

Virginia Commonwealth University
Richmond, Virginia
April, 2015

ACKNOWLEDGMENTS

First, I would like to thank my advisor Dr. Larisa Litovchick, for giving me an opportunity for working in her laboratory. She has been a constant source of motivation, a committed guide, who has shown me the right path and patiently answered all my questions throughout my tenure in her laboratory. I would also like to thank her for the numerous inputs throughout the journey of the compilation of this thesis. Her expertise in this field has helped me learn a lot more than what I could expect.

I thank my thesis committee members Dr. Andrei Ivanov and Dr. Diomedes Logothetis for their precious time invested in guiding me through this project. I express my sincere gratitude to them for their helpful advice and suggestions for improvising my project. A special thank you to Dr. Ivanov, for providing his expertise and helping us understand and interpret the experiment involving the actin cytoskeleton.

I thank Dr. Anton Chestukhin for letting me use the microscope at the translational research laboratory for acquiring immunostaining images.

I would like to thank all members of the Litovchick lab for their constant support. I express my sincere gratitude to Dr. Vijay Menon who has always been there to help me throughout the

duration of this project. I thank him for being so patient in teaching me immunostaining, transient transfections, testing of antibodies and for guiding me in troubleshooting my experiments. I thank Dr. Siddharth Saini for helping me with cyto-nuclear fractionations; Sophia Gruszecki, for preparing and making available all reagents used for this project and Jessica Felthousen for helping me whenever needed.

I thank Dr. Steven Grossman and his lab members for their varied inputs on my project. I also thank them for letting me use their microscope for quick expression analysis as well as acquiring images.

I would like to thank my friends, Ajinkya Kawale and Archana Bhat for being with me through all my highs and lows in these two years. Without the support of these two, the path would have definitely not been the same.

Last but not the least; I thank my parents and my brother who have been my support system all through, despite being miles apart. They have given me the strength to be away from home and pursue my dream that I have lived through this wonderful journey.

TABLE OF CONTENTS

LIST OF FIGURES

LIST OF ABBREVIATIONS AND SYMBOLS

2-D	2- dimensional
AD	Alzheimer's disease
ATCC	American type culture collection
BSA	Bovine serum albumin
CMGC	Cyclin dependent kinases, mitogen activated protein kinases, glycogen synthase kinases and CDC-like kinases
CRISPR	Clustered regularly interspaced short palindromic repeats
DAPI	4',6-diamidino-2-phenylindole
DCAF7	DBB1 and cullin associated factor 7
DIAPH1	Diaphanous-related formin 1
DMEM	Dulbecco's modified Eagle medium
DNA	Deoxyribonucleic Acid
DS	Down syndrome

DYRK	Dual specificity tyrosine related kinase
EDN1	Endothelin-1
EDTA	Ethylenediaminetetraacetic acid
FBS	Fetal bovine serum
GFP	Green fluorescence protein
GLI1	Glioma-associated oncogene 1
GTP	Guanine nucleotide tri phosphate
HIPK2	Homeodomain-interacting protein kinase 2
HRP	Horseradish peroxidase
IB	Immunoblot
IP	Immunoprecipitation
KD	KiloDalton
LATS2	Large tumor suppressor kinase 2
LZTS	Leucine zipper tumor suppressor
MALDI	Matrix assisted laser desorption/ ionization
mDia1/2	Mammalian diaphanous homolog 1/2
MEKK1	Mitogen-activated protein kinase kinase kinase 1
Mnb	Minibrain
MudPIT	Multidimensional Protein Identification Technology
N/ C terminal	Amino/ carboxy terminal

PAGE	Polyacrylamide gel electrophoresis
PBS	Phosphate buffered saline
PKN	Protein kinase N
pMSCV	Murine stem cell virus expression system plasmid
Puro	Puromycin
Rb	Retinoblastoma
RhoA	Ras homolog family member A
RNF169	Ring finger protein 169
ROCK	Rho associated protein kinase
RT	Room temperature
SDS	Sodium dodecyl sulfate
Ser	Serine
TAP	Tandem affinity purification
TBS	Tris buffered saline
Thr	Threonine
TOF	Time of flight
Tris- HCl	Tris hydrochloride
TROAP	Trophonin associated protein
USP7	Ubiquitin specific protease 7
VCM	Virus condition medium

WCE	Whole cell extract
WDR	Tryptophan- Aspartic acid repeat
WT	Wild type
β-ME	β-Mercaptoethanol
Δ	Deletion

ABSTRACT

UNDERSTANDING THE FUNCTION OF DYRK1A THROUGH CHARACTERIZATION OF ITS INTERACTING PROTEINS
By, Varsha Ananthapadmanabhan
B. Tech., D.Y Patil University, Navi Mumbai

A thesis submitted in partial fulfillment of the requirements of the degree of Master of Science at Virginia Commonwealth University.

Virginia Commonwealth University, 2015

Thesis Director: Larisa Litovchick, M.D., Ph.D.
Assistant Professor
Division of Hematology/Oncology and Palliative Care
Department of Internal Medicine

DYRK1A is a protein kinase encoded by a gene implicated in Down syndrome pathogenesis. Loss of DYRK1A could promote oncogenic transformation. However, the regulation and substrates of DYRK1A are not fully understood. MudPIT proteomic analysis revealed novel DYRK1A interacting proteins with poorly characterized or even unknown functions. Therefore, the aim of this thesis was to understand the function of DYRK1A through the characterization of

its interacting proteins. To achieve this aim, we established stable cell lines expressing these proteins and confirmed the interactions between DYRK1A and seven candidate binding partners. Furthermore, we found that all novel DYRK1A-interacting proteins also bind DCAF7, a previously reported DYRK1A-binding scaffold protein that binds to the N-terminus of DYRK1A. Using cyto-nuclear fractionation and immunostaining we found that DYRK1A-interacting proteins were present in different cellular compartments, suggesting that DYRK1A could play distinct roles in the cell depending on its localization. DYRK1A has been shown to regulate cell proliferation and actin cytoskeleton therefore we used cell proliferation assays and actin staining to determine the role of DYRK1A-interacting proteins in these processes. Here we report functional characterization of the interacting partners of DYRK1A and present cell-based models that will help to understand the function and regulation of this important protein kinase.

CHAPTER 1: INTRODUCTION

1.1. The DYRK kinases

The CMGC (cyclin dependent kinases, mitogen activated protein kinases, glycogen synthase kinases and CDC-like kinases) group of Serine/ Threonine kinases includes a conserved group of kinases called DYRK (Dual-specificity Tyrosine (Y) Regulated Kinases) (Alvarez *et. al*., 2007). The members of this enzyme family span across different species including *Drosophila*, yeast and mammals (Figure 1). It was found that the DYRK family members have striking similarities in their structural, functional and chemical characteristics (Becker and Joost, 1999).

This family can be sub- divided into two sub- families from a phylogenetic viewpoint: a group of cytosolic DYRK proteins, which includes *Schizosaccharomyces pombe* Pom1p, *Caenorhabditis elegans* mbk-2, *Drosophila melanogaster* dDYRK2, dDYRK3 and vertebrate DYRK2, DYRK3 and DYRK4; and a group of DYRKs that are considered mostly nuclear proteins, which includes *Saccharomyces cerevisiae* Yak1p, *Dictyostelium discoideum* YakA, *C.*

elegans mbk-1, *D. melanogaster* minibrain, and vertebrate DYRK1A and DYRK1B (Alvarez *et al*., 2007).

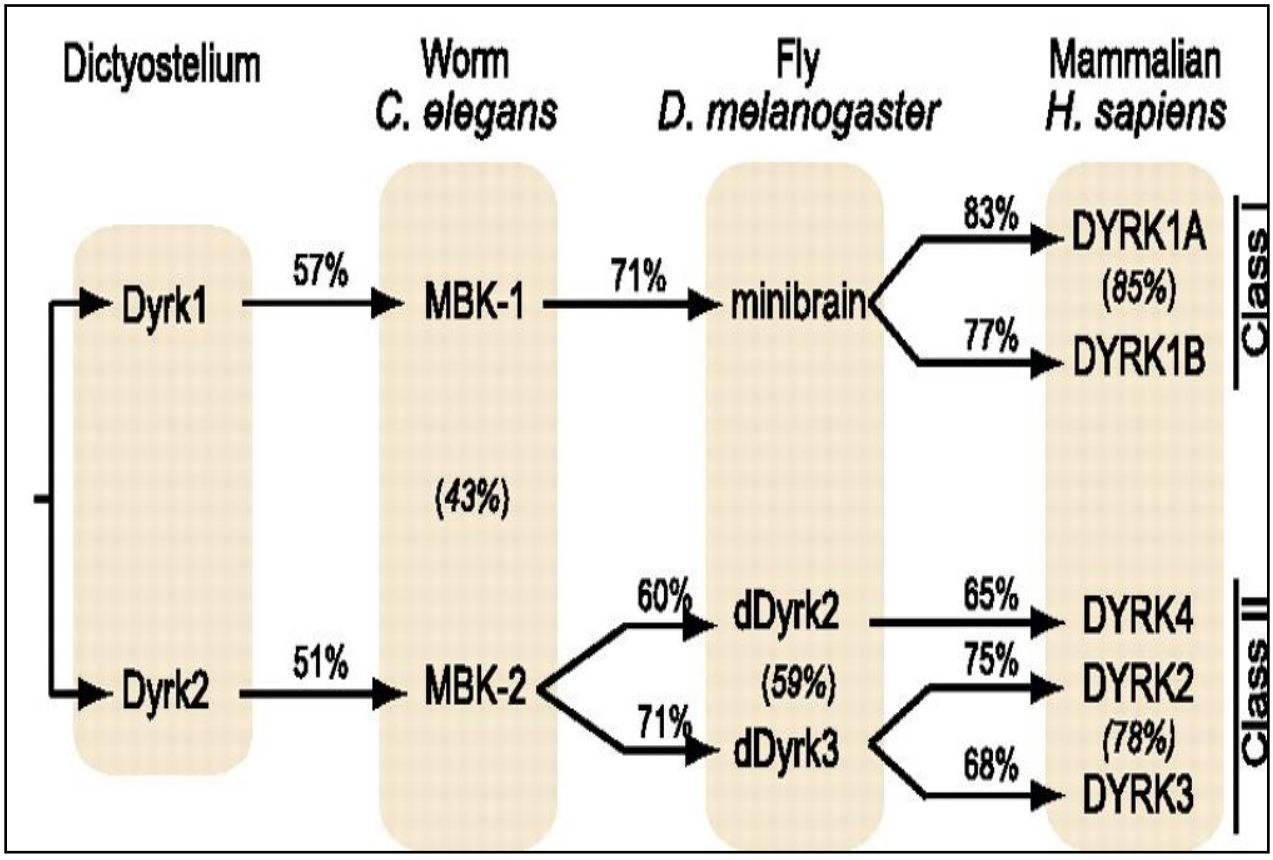

Figure 1: Phylogenetic tree of the DYRK family. DYRK subfamily members can be classified into 2 main groups: class I and class II. The percentage of conservation at the protein level between orthologues is indicated above the arrows and between 2 paralogues is indicated in parentheses within the boxes. The phylogenetic classification correlates to the functional classification of the DYRK subfamily as class I and class II kinases. (Adopted from Aranda, Laguna and de la Luna, 2010)

Mammalian DYRK kinases include two nuclear proteins, or Class I (DYRK1A and DYRK1B) as well as three cytosolic members or Class II (DYRK2, DYRK3 and DYRK4) (Fig. 2). DYRK1A and DYRK1B are the closest homologs of the *Drosophila* Mnb gene.

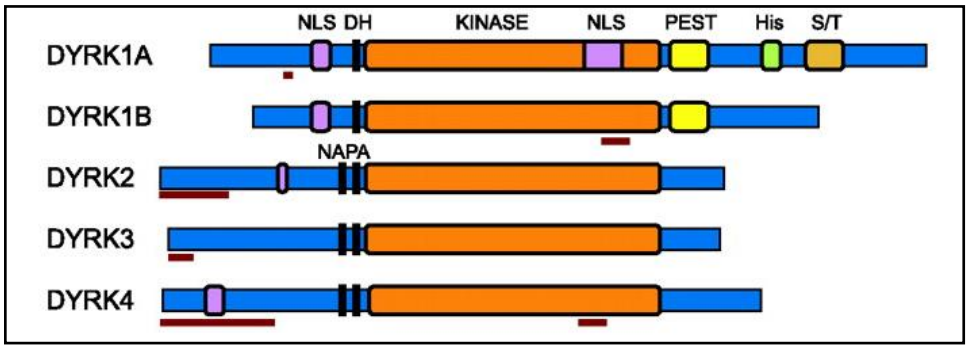

Figure 2: Schematic representation of the domain structure of the 5 mammalian DYRKs. The known protein motifs are indicated by different colors. Red lines indicate protein regions affected by alternative splicing events (Adopted from Aranda, Laguna and de la Luna, 2010).

All mammalian DYRKs share a DH-box or DYRK homology domain (DDDNXDY) that is adjacent to a highly conserved kinase domain with less sequence similarity in the N- and C-terminal regions (Figure 2) (Alvarez *et. al*., 2007). All members of this family are characterized by a conserved Tyr-X-Tyr motif in the activation loop of the catalytic domain (Becker and Joost, 1999). Phosphorylation of the second tyrosine residue during protein folding is required for the activation of all known DYRK family members (Himpel *et al*., 2001; Li *et al*., 2002; Lochhead *et al*., 2003). It was reported based on studies with *Drosophila* DYRKs that this phosphorylation event occurs in cis during the translation of the nascent enzyme. Mature DYRKs lose their tyrosine phosphorylation activity and retain only serine/threonine phosphorylation ability (Lochhead *et al.*, 2005). Hence, DYRKs phosphorylate themselves at tyrosine residues and phosphorylate their substrates at serine/ threonine residues (Becker and Joost, 1999).

1.2. DYRK1A

The mammalian DYRK1A is ubiquitously expressed in adult and fetal tissues (Guimera *et al*., 1999; Okui *et al*., 1999). In addition to the conserved catalytic kinase domain (Figure 2), DYRK1A has two nuclear localization signal sequences (NLSs): a classical bipartite NLS at the N terminal region of the protein and a complex NLS within the catalytic domain (Alvarez *et al*., 2003). The kinase domain is followed by a PEST domain and then by a histidine-rich domain that targets DYRK1A to the nuclear speckles compartment where it may co-localize with splicing machinery (Figure 2) (Alvarez *et al*., 2003).

Several reported substrates of DYRK1A harbor a consensus sequence that includes RPX(S/T) P motif. Analysis of the *in vitro* phosphorylated synthetic peptide substrates established DYRK1A's preference for arginine residue in -2 or -3 position and for a proline at the +1 position (Himpel *et al*., 2000, 2001).

1.3. Role of DYRK1A in development

Analysis of the Mnb mutants in *Drosophila* provided the initial evidence for the involvement of the *Drosophila* homolog of DYRK1A in neural proliferation and differentiation since the loss-of-function Mnb flies developed a smaller adult brain. This phenotype was most prominently observed in the optic lobes (Tejedor *et. al*., 1995).

Similarly, DYRK1A is essential for mammalian embryonic development. Fotaki *et. al*. reported a significant growth delay in Dyrk1a$^{-/-}$ mouse embryos. They reported a 25% to 50% reduction in the body size of the mice (2002). These mice died between embryonic day 10.5 and embryonic day 13.5. Reduced postnatal viability was also reported in case of Dyrk1a$^{+/-}$ mice

wherein 29% of the Dyrk1a haploinsufficient mice died during the first 3 days of life, along with having reduced body weight, brain size and total number of neurons (Fotaki *et. al*., 2002). It was also observed that truncation of the DYRK1A gene due to cytogenetic aberrations in humans caused microcephaly, severe mental retardation and other developmental abnormalities (Moeller *et. al*., 2008). This evidence strongly suggests that DYRK1A plays a vital role in brain and body development (Moeller *et. al*., 2008).

1.4. Role of DYRK1A in Down syndrome and neurodegenerative disorders

Congenital Down syndrome (DS) most frequently arises due to an error in maternal non-disjunction during meiosis that results in the presence of three full copies of human chromosome 21. DS also occurs in people carrying unbalanced translocations, which result in the triplication of only a part of chromosome 21. By correlating phenotype with genotype in patients with partial trisomies, a ch21 region named the DSCR (Down syndrome critical region) has been defined. The DSCR, when present in three copies, is responsible for many of the characteristic features of DS. DYRK1A is located in the ‘‘Down syndrome-critical region’’ on chromosome 21q22.2 and is thought to play a role in the aberrant brain development, lifelong structural and functional neurological abnormalities, neural degeneration and neuronal death (Guimera *et. al*., 1996; Tejedor and Hammerle, 2011; Wegiel *et al.*, 2011). It was suggested that DYRK1A overexpression could contribute to the depletion of neurons in the developing brain of the DS fetuses in two ways: firstly, the overexpression of DYRK1A may cause the precocious onset of neurogenesis in progenitors and lead to the concomitant depletion of the proliferating progenitor pool. Secondly, due to its role in regulating the cell cycle exit of neurons, overexpression of

DYRK1A may induce a premature cell cycle arrest of the neurogenic progenitors leading to a decrease in the number of neurons generated by each progenitor (Tejedor and Hammerle, 2010).

Although over-expressed DYRK1A localizes to the nucleus, close to 75% of the endogenous DYRK1A protein in the human brain is associated with an insoluble cytoskeletal fraction while the rest is divided between the nucleus and a soluble cytosolic fraction (Kaczmarski *et al.*, 2014). Therefore, overexpression of DYRK1A in DS and other disorders may produce cell compartment–specific changes that could result in altering brain development, maturation and susceptibility to neurodegeneration (Wegiel *et al*., 2011). Indeed, an increase in the DYRK1A immunoreactivity has been reported in Down syndrome, Alzheimer's disease (AD) and Picks disease (Ferrer *et. al*., 2005 and Wegiel *et al*., 2011).

It has also been reported that DYRK1A can contribute to several forms of neurodegeneration, including α-synuclein aggregation and fibrillization in Lewy bodies, granulovacuolar degeneration in the hippocampal pyramidal neurons as well as in age-related or AD- and DS/AD-related neuronal and astrocyte degeneration with DYRK1A-positive corpora amylacea, (Wegiel *et. al*., 2011). DYRK1A could contribute to phosphorylation of the human microtubule-associated protein Tau at 11 known sites. These sites are significantly hyper phosphorylated in the DS brain, leading to the reduction of the biological function of Tau due to increased self-aggregation and fibrillization, ultimately causing neuronal death. The microtubule assembly is also compromised (Liu *et. al*., 2007 and 2008; Wegiel *et. al*., 2011), possibly contributing to dendritic shortening and atrophy in DS (Tejedor and Hammerle, 2010). Moreover, Wegiel *et. al*., reported that DYRK1A-positive neurofibrillary tangles (*NFTs*, comprised of the aggregates of hyper phosphorylated tau protein), were found in 60% of the spontaneous Alzehimers disease

patients as well as in all DS patients who developed AD (2011). Increasing contribution of DYRK1A with age to the progression of neurofibrillary degeneration in DS subjects has been observed. However, in sporadic AD, the percentage of DYRK1A-positive NFTs does not change with age or disease duration, suggesting the extra dosage of DYRK1A can contribute to the early onset of AD (Wegiel *et. al*., 2008).

Given that increased expression and activity of DYRK1A contributes to the neurological abnormalities in DS and AD, targeting DYRK1A for therapy could help to alleviate the mental retardation associated with these conditions.

1.5 Role of DYRK1A in the cell cycle

Cells have to progress through the different cell cycle phases for proliferation and exit the cell cycle in order to undergo differentiation. In the absence of the growth signals, the cells exit the cell cycle and enter the G_0 or quiescence state. This is important for cell differentiation, development of tissues and prevention of tumorigenesis. Inactivation of factors that control the ability of cells to enter the G_0 state results in increased proliferation, tumor formation as well as defects in differentiation (Malumbres and Barbacid, 2001; Vidwans and Su, 2001; Massague, 2004; Koreth and van den Heuvel, 2005; Miller *et al*., 2007; Litovchick *et. al*., 2011).

Several reports implicate DYRK1A into regulation of cell proliferation. In *Drosophila*, both Minibrain and dDYRK2 interact with the chromatin remodeling factors SNR1 and TRX and hence play a role in cell cycle regulation (Kinstrie R *et. al*., 2006). In a study by Branchi *et. al*., it was reported that transgenic mice overexpressing DYRK1A have increased levels of cyclin B (2004). Another study found that in neurogenic mouse epithelia, DYRK1A promotes the nuclear

export and degradation of cyclin D1 leading to premature differentiation of neural progenitor cells to neurons (Yabut *et al*., 2010). Using the chick embryonic spinal cord and mouse telencephalon models, it was demonstrated that a transient expression of MNB/DYRK1A in neuronal precursors acts as a binary switch, coupling the end of proliferation and the initiation of neuronal differentiation by up regulating $p27^{KIP1}$ expression and suppressing the Notch signaling (Hammerle B *et. al*., 2011). Furthermore, Park *et. al*., demonstrated that DYRK1A-induced p53 phosphorylation at Ser15 led to a robust induction of p53 target genes such as $p21^{CIP1}$ and impaired $G1/G_0$-S phase transition, resulting in attenuated proliferation of H19-7 cells and human embryonic stem cell derived neural precursor cells (2010). Soppa *et*. *al*. demonstrated that DYRK1A promotes the cell cycle exit by phosphorylating Thr286 in cyclin D1 that targets this protein for proteasomal degradation, and by phosphorylating Ser10 in $p27^{Kip1}$, resulting in protein stabilization (2014). A recent chromatin-wide profiling of DYRK1A revealed that DYRK1A could act as a RNA Polymerase II CTD kinase in order to facilitate transcription of certain RNA Polymerase II target genes. According to the proposed model, DYRK1A is recruited to its target genes after recognizing the motif TCTCGCGAGA. This is followed by phosphorylation of the CTD of RNA Pol II at Ser2 and Ser5 (Vona *et. al*., 2014).

The activity of E2F transcription factors is regulated by the retinoblastoma (RB) family of proteins that includes pRB, p107 and p130. The Rb family proteins act as tumor suppressors in a hypo-phosphorylated form when they bind E2F transcription factors and inhibit the E2F-mediated transcription. Cyclin-dependent kinases (CDKs) phosphorylate these RB family members in a cell cycle-dependent manner to relieve the binding and inhibition of E2Fs (Cobrinik, 2005; Malumbres and Barbacid, 2009). It was revealed through mouse genetic studies

that the RB family proteins perform redundant functions to control entry into the G0/G1 state whereby any one of the RB-like proteins can compensate for loss of the others. However, only a partial redundancy is seen in the embryonic development and tumor suppression whereby pRB has unique functions (Cobrinik, 2005; Dannenberg and te Riele, 2006). Despite the redundant functions in G0/G1, accumulation of p130 is observed in response to serum starvation, confluency or p^{INK4a} expression in the cells entering quiescence (Smith *et al*. 1996; Cam *et al*. 2004). Furthermore, p130 was found to be the predominant RB family member that interacts with MuvB core protein complex consisting of RBBP4, LIN9, LIN37, LIN52 and LIN54. Mass spectroscopy proteomic analysis in human cell lines revealed that p130 interacts with E2F4, DP1 and the MuvB core forming the DREAM complex in G0/G1 but not in the S-phase and subsequently causes repression of the DREAM target genes (Litovchick *et al*. 2007; Schmit *et al*. 2007). In the S phase, the MuvB core dissociates from the p130-DREAM and binds BMYB in order to cause transcription of the MMB (MYB-MuvB) target genes (Litovchick *et. al*., 2007; Schmit *et. al*., 2007).

Studies by Litovchick *et. al*. reported that DYRK1A specifically phosphorylates the serine 28 residue on LIN52 (Figure 3). This phosphorylation was found to be required for DREAM assembly. Point mutation of LIN52 or inhibition of DYRK1A activity disrupts DREAM assembly and reduces the ability of cells to enter quiescence or undergo Ras-induced senescence (Litovchick L *et. al*., 2011).

Thus, DYRK1A has been found to play an important role in the regulation of DREAM activity and entry into quiescence.

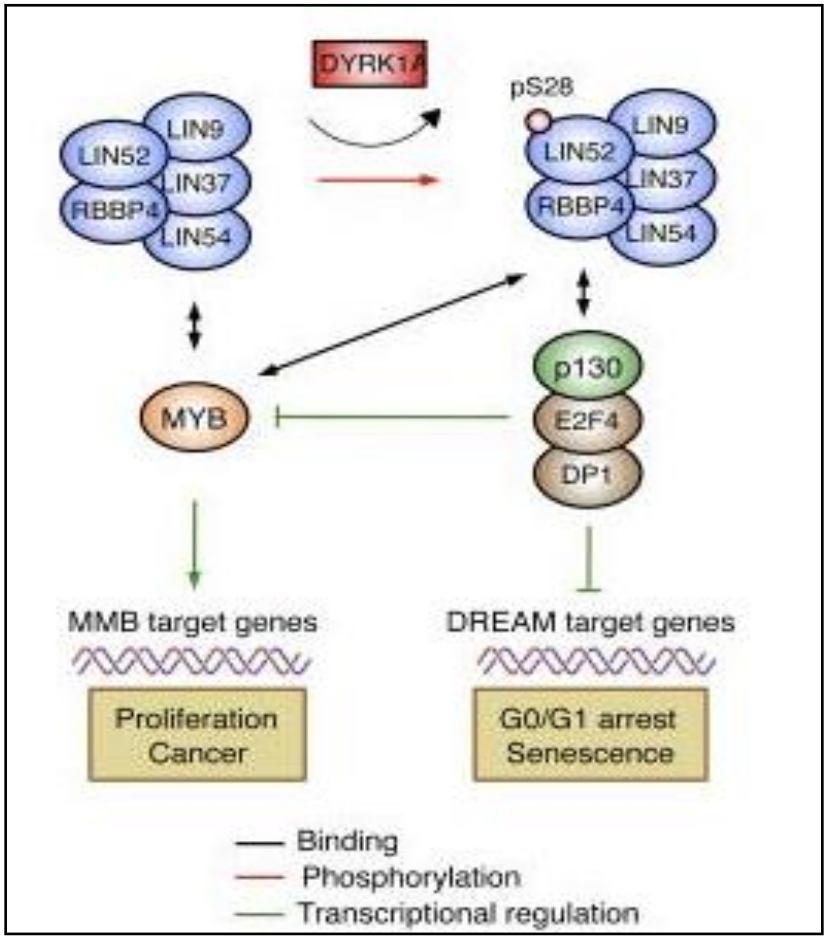

Figure 3: **A model depicting how DYRK1A promotes the DREAM complex assembly, G0/G1 arrest, and senescence** (Adopted from Litovchick *et. al*, 2011)

1.6. DYRK1A and the Hippo pathway

The Hippo signaling pathway is involved in the control of cellular proliferation and organ size and its main components are conserved between drosophila and humans (Harvey *et. al*., 2013). More than 35 proteins have been identified in the human Hippo pathway. In figure 4, putative oncoproteins are shown in red and putative tumour suppressors are shown in blue (Harvey K F

et. al., 2013). The Yes-associated protein (YAP) is a homolog of the Yorkie protein in Drosophila. Transcriptional activity of YAP is controlled by upstream regulatory proteins in response to cell density. When the cell density is high and the cells are closely packed with each other, the kinases MST1 and MST2 are activated. These in turn phosphorylate and activate LATS2 (Large Tumor suppressor-2) which phosphorylates YAP. The phosphorylation of YAP causes its retention in the cytoplasm and subsequent degradation. On the other hand, when the cell density is low, YAP is free to translocate into the nucleus. In the nucleus, this protein with PDZ-binding motif (TAZ) activity acts as a transcriptional co-activator causing the transcription of various genes required for cell proliferation (Harvey *et. al.*, 2013).

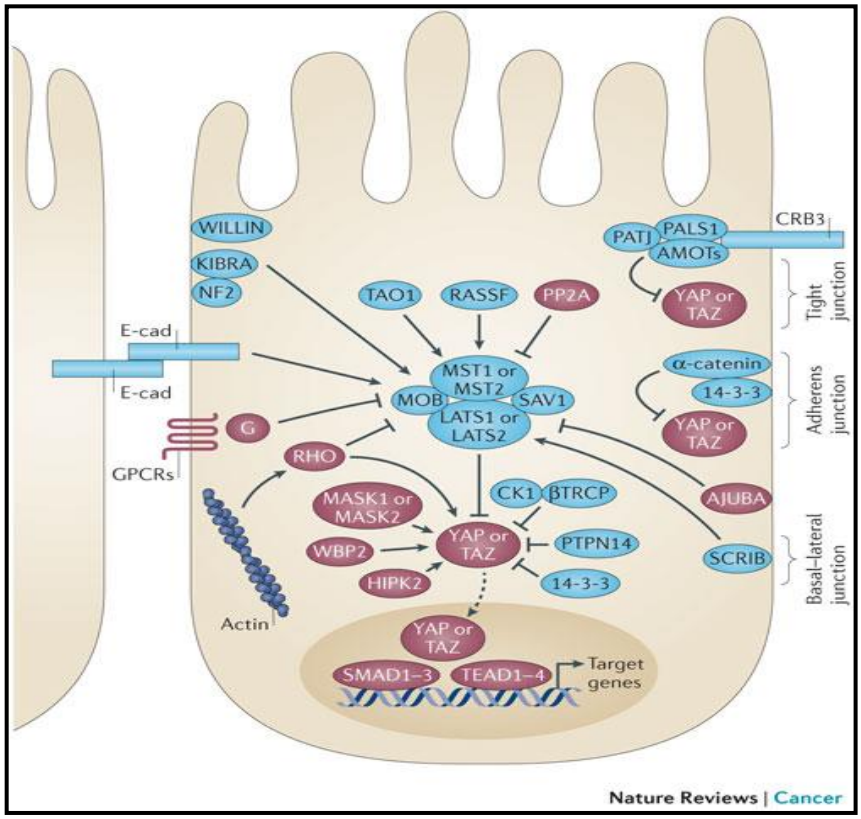

Figure 4: A schematic diagram of the mammalian Hippo pathway (Adopted from Harvey *et. al.*, 2013).

Intriguingly, experimental evidence suggests that DYRK kinases could be a part of the Hippo pathway. Using an *in vitro* kinase assay system Tschop *et al.* demonstrated that LATS2 could phosphorylate and activate DYRK1A's ability to phosphorylate LIN52 (Figure 5) (2011). In the same study, both LATS2 and DYRK1A were required for the DREAM-mediated repression of its target genes. However, genetic studies in Drosophila (Degoutin *et al*., 2013) resulted in a different model in which Mnb (DYRK1A) was proposed to serve as an upstream negative regulator of Wts (LATS). Therefore, it is important to further investigate the functional relationship between DYRK1A and LATS in various experimental systems.

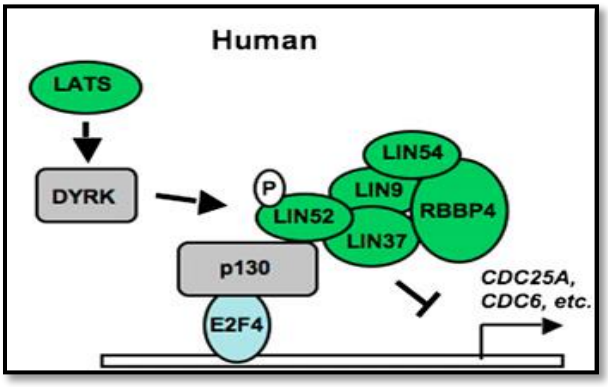

Figure 5: **The proposed LATS-DYRK1A-DREAM signaling cascade** (Adopted from Dick and Mymryk, 2011).

1.7 Proteomics approaches to characterize DYRK1A

Proteomics approaches identify the protein-protein interactions usually by using the Mass-spectrometry analysis of the immunoprecipitated (or immunoaffinity purified) epitope-tagged protein of interest. Traditional proteomic analysis involves the separation of protein samples using one- or 2-Dimensional (2-D) electrophoresis, extraction of proteins of interest from the gel

and the MALDI-TOF analysis. The comparison of the measured peptide masses obtained with theoretical predicted values present in databases is required in order to determine the correct protein mass based on the number of statistically significant matches (Schirmer, 2009).

Multidimensional Protein Identification Technology (MudPIT) does not require gel separations that are needed in the traditional mass-spectroscopy (Link and Washburn, 2014). In MudPIT, biochemical fractions containing many proteins obtained from immunoprecipitates, are directly proteolysed. The peptide mixtures are first subjected to 2-D liquid chromatography and then to an electrospray ionization tandem mass spectrometry (ESI-MS/MS). The peptide is fragmented using a collision-induced dissociation cell and the masses of the fragmentation products are determined. Bioinformatics tools can transform these data into an amino acid sequence. In a typical analysis, thousands of peptides can be confidently identified from a sample (L. Litovchick, personal communication). Thus, the MudPIT technique has an advantage of being highly sensitive over the traditional 2-D gel method (Schirmer, 2009).

MudPIT approach was applied for the proteome analysis of the human CMGC group of kinases (including DYRK1A) carried out by Varjosalo *et al*. (2013). Using HEK 293T cells, it was reported that the DYRK sub network is composed of 60 proteins and 78 interactions. Most of the interactions found in this study constituted complexes containing the highly related class I family members DYRK1A and DYRK1B. DYRK1A and DYRK1B complexes had 20 proteins in common, and these proteins were not found in complexes with the class II family members. The observed differences were consistent with the idea that class I and class II DYRKs have undergone functional diversification by acquiring new protein interactions as they diverged early in evolution (Aranda *et al*., 2010).

Additional MudPIT analysis by Litovchick L *et. al.* (personal communication), revealed fifty proteins that specifically and reproducibly interacted with DYRK1A in T98G glioblastoma cell line. Most of the interacting proteins found through this analysis in T98G cells overlapped with the analysis by Varjosalo *et al*., using HEK 293T cells. Out of the four biological repeats of the analysis conducted, six proteins were found to interact with DYRK1A in all the four repeats. They were DCAF7, FAM117A, FAM117B, LZTS2, TROAP and RNF169 (L. Litovchick, unpublished data, and Figure 6). Among the proteins identified as DYRK1A interacting proteins in three out of the four repeats, we noted LZTS1 (a homologue of LZTS2) and USP7 protein involved in the ubiquitin-regulated processes. Interestingly, most of the DYRK1A interacting proteins are not very well characterized while others have some previously attributed functions that are described below.

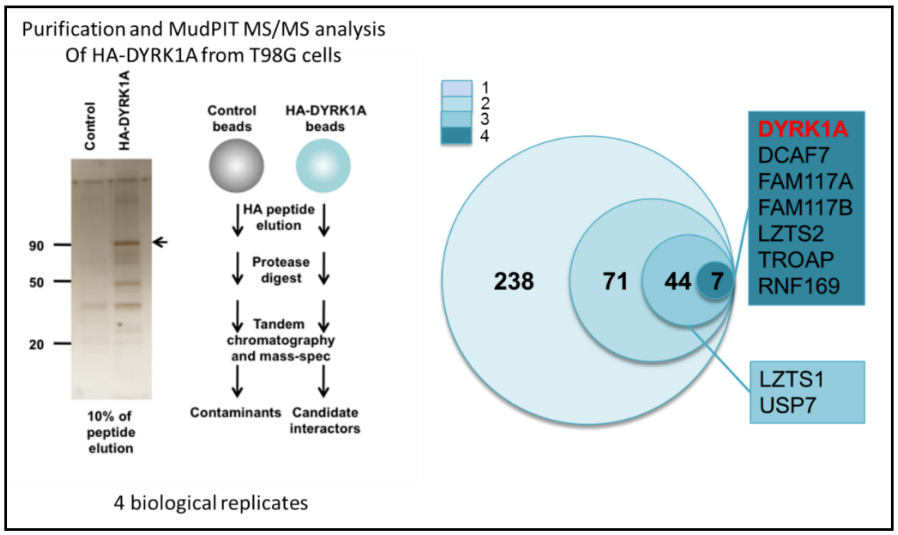

Figure 6: Identification of DYRK1A interacting proteins (by L. Litovchick, personal communication).

1.8 DCAF7

WDR68 (WD-repeat protein 68) was originally identified in petunia as a gene (AN11) located in a locus that controls the pigmentation of flowers by stimulating the transcription of anthocyanin biosynthetic genes (Jin *et. al.*, 2006). The orthologues of this gene have been identified in many species (Jin J *et. al.*, 2006). The amino acid sequence of human AN11 (HAN11) has 52% amino acid identity with petunia AN11, and is 100% identical with that of monkey, mouse, rat, dog, cow, and chicken (Jin *et. al.*, 2006). It is not clear if the petunia AN11 and HAN11 have conserved functions. AN11 and its orthologues all encode a protein with five WD40-repeats that is structurally related to the DDB1 ubiquitin ligase and Cullin associated protein factors. Hence it was officially renamed as DDB1 and Cullin associated factor 7 or DCAF7 (Lee, 2007). Along with over 60 other DCAFs, DCAF7 is predicted to act as a substrate receptor for the DDB1-Cullin complexes although this function has not been experimentally demonstrated.

Using yeast two-hybrid screening, DCAF7 was found to act as a scaffold receptor to control HIPK2 and MEKK1 kinase functions (Ritterhoff, et al. 2010). Using co-immunoprecipitation experiments, both DYRK1A and DYRK1B have been found to bind DCAF7 protein (Skurat and Dietrich, 2004). There is evidence that DCAF7 binds DYRK1A and this binding induces the nuclear translocation of the predominantly cytosolic protein DCAF7 (Miyata., 2011). This demonstrates that DYRK1A could have a role in the localization of its interacting proteins. The N-terminal region of DYRK1A has been found essential for its binding to DCAF7. On the other hand, WD40 repeats alone are not sufficient for the binding of DCAF7 to DYRK1A. It was found that the N and C terminal regions are also needed for the binding (Miyata, 2011). DCAF7 also interacts with mDia1 (DIAPH1) and controls GLI1 transcriptional activity (Morita *et al.*, 2006). This conserved protein plays a role in craniofacial development upstream of the EDN1

pathway (Nissen *et al*., 2006). Physiological role of DCAF7 is not yet understood although there is evidence that it could be required for cellular proliferation (Miyata Y, 2011 and Ritterhoff , *et al*. 2010) and osmotic stress response (Ritterhoff , *et al*., 2010).

1.9 LZTS1

The Leucine Zipper putative Tumor Suppressor 1 (LZTS1, also known as FEZ1) gene was identified as a tumor suppressor gene at the 8p22 locus (Ishii *et. al*., 1999). The protein LZTS1 is ubiquitously detected in normal tissues but is frequently downregulated or absent in different human cancers (Francesca L *et. al*., 2013). LZTS1 deficient mice develop cancers with diverse histogenetic backgrounds suggesting that LZTS1 acts as a major tumor suppressor gene in multiple cell types (Baffa R *et al*., 2008). This protein inhibits cancer cell growth through the regulation of the mitotic process. It may also have a role in cell cycle control by interacting with the Cdk1/cyclinB1 complex (Vecchione *et. al*, 2007). It is thought to act by stabilizing the Cdc25C phosphatase, a mitotic activator of Cdk1 (Vecchione *et. al*, 2007). The role of LZTS1 with regard to DYRK1A is not characterized. It is particularly interesting to determine if LZTS1 acts as a tumor suppressor in all cell types and if it does then does it contribute to the tumor suppressive ability of DYRK1A.

1.10 LZTS2

LZTS2 (or LAPSER1) is an LZTS1-related gene that encodes a protein that shares 37% identity with LZTS1. LZTS2 has been mapped to a sub-region of human chromosome 10q24.3, which is deleted in various cancers, along with its neighboring PTEN locus (Cabeza-Arvelaiz *et. al*., 2001). Overexpression of LZTS2 cDNA strongly inhibits cell proliferation and the colony

forming efficiencies of most cancer cells (Cabeza-Arvelaiz *et. al*., 2001). This includes LNCaP, TRSUPr1, PC3, U2OS, HEK-293T, AT6.2, and Rat-1 cells suggesting that the LZTS2 gene is also involved in the regulation of cell proliferation (Cabeza-Arvelaiz *et. al*., 2001). The loss of LZTS2 function may contribute to cancer development (Cabeza-Arvelaiz *et. al*., 2001). Hence, similar to LZTS1, LZTS2 is an interesting candidate that could mediate the role of DYRK1A in regulation of cell proliferation. While the function of LZTS2 is not fully understood, evidence points to its involvement into several cancer-related pathways. Increased nuclear localization of β-Catenin due to aberrant activation of the Wnt pathway contributes to cancer. LZTS2 interacts with β-Catenin and regulates its nuclear export, thus increasing the cytosolic pool of β-Catenin (Thyssen *et. al*., 2006). Furthermore, LZTS2 was seen to inhibit cell proliferation and regulate Lef/Tcf-dependent transcription through Akt/GSK3β signaling pathway in lung cancer (Cui *et. al*., 2013). LZTS2 is also required for central spindle formation and the completion of cytokinesis (Sudo *et. al*., 2008). Finally, the protein interaction network of the mammalian Hippo pathway revealed interaction of LZTS2 with LATS2 (Couzens *et. al*, 2013). Thus, this DYRK1A interacting protein found through the proteomic analysis could provide a connection between the Hippo pathway and DYRK1A.

1.11 USP7

Herpes virus-associated ubiquitin-specific protease (HAUSP), also known as ubiquitin-specific protease 7 (USP7), is a deubiquitinating enzyme that removes ubiquitin moieties from target proteins such as p53 and MDM2 (Vogelstein *et al*., 2000). USP7 also regulates the cellular localization of the oncogenic transcription factor FOXO4, and the tumor suppressor phosphatase PTEN through its deubiquitinating activity (Song *et al*., 2008, Trotman *et al*., 2007 and van der

Horst *et al*., 2006). It is also thought to play a role in UV induced excision repair. The interaction of DYRK1A with USP7 could reveal a previously unknown function of DYRK1A.

1.12 RNF169

RNF169 is a protein recruited to the double strand break (DSB) DNA repair sites by recognizing and binding ubiquitinated histones. Human RNF169 is a negative regulator of the ubiquitin-dependent response to DNA double-strand breaks catalyzed by RNF8 and RNF168. By structural homology with RNF168, RNF169 could function as E3 ubiquitin-protein ligase although this activity could not be detected *in vitro* using purified histone as substrate (Poulsen *et al*., 2012). Interaction between RNF169 and DYRK1A has been confirmed both at the overexpressed and the endogenous levels (unpublished data from Dr. Vijay Menon, Litovchick lab) and the role of DYRK1A in regulation of RNF169 is currently under investigation.

1.13 TROAP

The protein TROAP (originally called Tastin) is a protein that forms a complex with trophinin and bystin. Hence it was renamed as Trophinin associated protein (TROAP). This complex is required for the initial adhesion of the blastocyst to uterine epithelial cells at the time of the embryo implantation. This is accompanied by rapid cellular invasion and proliferation (Fukuda., and Nozawa., 1999). Although TROAP expression is absent in most adult tissues (Nadano *et. al*., 2002), higher levels of expression are observed in testis, bone marrow and thymus as well as human cancer cell lines such as HeLa and Jurkat cells (Genomics Institute of the Novartis Research Foundation [GNF] database). In mammalian cells, TROAP is thought to associate with the microtubules (Nadano, et. al., 2002). Considering that TROAP is expressed in multiple

tissues and cells unrelated to embryo implantation, it is possible that TROAP has additional functions. One of its functions is its requirement for bipolar spindle assembly and centrosome integrity during mitosis (Yang S, *et al*., 2008). This function of TROAP is poorly understood but its association with microtubules makes it an interesting candidate that could elucidate the role of DYRK1A in mitosis and cell morphology.

1.14 FAM117B

FAM117B, also known as ALS2CR13 is an Amyelotropic Lateral Sclerosis (ALS) candidate gene (RefSeq data). This is a protein with unknown function.

In summary, despite the important physiological role of DYRK1A and its involvement in human disease, the regulation and substrates of this protein kinase are not very well understood. Proteomic analysis of DYRK1A-interacting proteins revealed a number of interesting candidates, most of which are not functionally characterized yet. Therefore, the goal of this study was to understand the function of DYRK1A through initial characterization of some of its interacting proteins.

CHAPTER 2: MATERIALS AND METHODS

2.1 Cell culture

Established T98G, U-2 OS, HEK-293 and Phoenix cell lines were obtained from ATCC. The cells were grown under sterile conditions in a 37°C incubator with 5% CO_2 in the Dulbecco's modified medium (DMEM, Corning Cat# 15-013-CV) supplemented with 1% (v/v) GlutaMax (Life Technololgies, Cat# 35050-61), 1% (v/v) Penicillin/Streptomycin (Corning, Cat# 30-002-CI) and 10% (v/v) FBS (Atlanta Biology, Cat# S11150). For passaging, the cells were washed twice with 1X PBS (Corning, Cat# MT21-031-CV), detached using 0.25% Trypsin/EDTA (Gibco, Cat# 25200-056) followed by re-suspension in fresh growth medium. The cells were counted using a hemocytometer (Hausser Scientific) and seeded into p100, 6-well or 12-well tissue culture plates according to the experimental protocols.

2.2 Cloning of constructs into pMSCV backbone

The tandem affinity purification (TAP, or HA-Flag) -tagged GFP, DYRK1A, DCAF7, LZTS2, LZTS1, FAM117B, TROAP and USP7 constructs were prepared using Gateway recombination cloning Clonase II kit (Life Technologies) according to the manufacturers protocol. Entry clones

were obtained from Harvard PlasmID repository while the retroviral pMSCV-CTAP-Puro and pMSCV-NTAP-Puro Gateway destination vectors were a gift from M. Sowa.

2.3 Production of retroviral particles

DNA vectors containing the target sequence inserted into pMSCV-CTAP or -NTAP retroviral vectors were used for the production of virus condition medium (VCM) by transfecting Phoenix packaging cells. For each plasmid to be transfected, 200,000 cells were plated in each well of a six well plate in complete 2.5mL of DMEM medium and allowed to attach overnight. When the cells attained approximately 80% confluency, they were transfected with 2 µg of pMSCV plasmid containing the gene of interest together with 0.1 µg pCMV-GagPol packaging plasmid and 0.1 µg pCMV-VSVG envelope plasmid. OptiMEM medium (Life Technologies, 31985070) and TransIT2020 Mirus reagent (Mirus Bio, Cat# MIR 5400) were used for the transfection according to the manufacturer's protocol. The VCM was collected 48 and 72 hours post transfection and centrifuged at 2000rpm at 4°C for 10 minutes to collect the supernatant devoid of the Phoenix cells. Aliquots of the VCM were made and stored at -80°C.

2.4 Generation of stable cell lines

The VCM was allowed to thaw overnight at 4°C and centrifuged at 14,000g for 10 minutes at 4°C. T98G cells (50,000 cells per well in a 12-well plate) were plated and allowed to attach overnight. On the next day, the medium was aspirated from each well and replaced with 500µL of fresh medium containing polybrene (8µg/mL) (Sigma, Cat# 107689) and 500µL of VCM. The medium was replaced next day with 1mL of fresh complete DMEM medium per well. On the following day, the cells were subjected to antibiotic selection by changing the medium to

medium containing 1µg/mL Puromycin (Gold Biotechnology, Cat# P-600-100). The selection process was continued for 1 week.

2.5 Preparation of cell extracts

Cell lysates were typically obtained when the cells become confluent. The cells from p100 were rinsed twice with PBS and then scraped into 0.5mL of ice cold PBS containing protease inhibitor cocktail at a dilution of 1: 100 (Calbiochem, Cat#539131) and phosphatase inhibitors at a dilution of 1: 500 (Calbiochem, Cat# 524625). The cells were collected by centrifugation and the pellets were either frozen at -80°C for further analysis or lysed immediately. The lysis was performed using EBC buffer (50 mM Tris-HCl pH 8.0, 5mM EDTA, 120 mM NaCl and 0.5% NP-40) supplemented with protease inhibitors (1:100), phosphatase inhibitors (1:500) and β-ME (1:10,000). The lysates were clarified by centrifugation (14,000g, 15min) and the protein concentrations were measured using the BioRad DC assay.

2.6 Immunoprecipitation

The cell extracts were normalized to contain the same amount of protein. An 50-100µL aliquot of each lysate used to prepare the Input sample by mixing with equal volume of 2X SDS PAGE sample loading buffer (BioRad, Cat# 161-0737) and incubating at 95°C for 5 min. A mixture containing 1µg of antibody, 20µL of Protein A Sepharose beads suspension (GE healthcare, Cat# 17-0780-01) and 80µL of PBS was added to the lysates and incubated overnight on a rocker at 4°C. The next day the beads were collected by centrifugation at 10,000g for 15 sec at 4°C and washed five times with cold EBC buffer to remove any unbound protein. After the last wash, the

supernatant was aspirated and 35µL of 1X SDS PAGE sample loading buffer was added to the tubes followed by incubation of the tubes at 95°C for 5 min.

2.7 Western Blotting

The samples for Western blot analysis were resolved using a 10% SDS-PAGE gels or the Any-kD ready-made gels (BioRad Cat# 4569034) and transferred to a nitrocellulose membrane (Amersham, Cat# 10600006) using semi-dry electrophoretic transfer (40 min, 15V). The membrane was blocked for 1 hour in 3% non-fat dry milk in TBST buffer containing 1X Tris buffered saline (TBS) (Boston BioProducts, Cat# BM-300) and 0.05% Tween-20 (BioRad Cat# 1610781). The membranes were then probed with primary antibodies diluted in the blocking buffer and incubated overnight at 4°C. The blots were developed by incubation with horseradish peroxidase (HRP) -conjugated secondary antibodies (anti-rabbit or anti-mouse) diluted in 1% milk for one hour at room temperature followed by chemiluminescence detection. Protein bands were visualized using X-ray film (Phenix, Cat# F-BX57 and F-BX810) or the Bio-Rad multi-imager (ChemiDoc MP). If re-probing of the blots was required, the Restore Western reagent (Thermo Scientific, Cat# 46430) was used for stripping the membranes.

2.8 Antibodies

Anti-HA antibody (clone 12CA5) used for pull down experiments was a hybridoma supernatant kindly provided by J. A. DeCaprio. The mouse anti-HA antibody (HA.11, Covance MMS- 101P) or the rabbit anti-HA antibody (Cell Signaling, Cat# 3724S) were used for Western Blot Analysis of HA-tagged proteins. For DYRK1A pull down experiments and for immunoblotting, the rabbit anti-DYRK1A antibody (Bethyl, Cat# A303-801A) was used. The mouse anti-

DYRK1A antibody (Sigma, Cat# WH0001859M1) was used only for immunoblotting analysis. The non-targeting rabbit IgG (Bethyl, Cat# P120-101) antibody was used for pull down controls. Samples of rabbit antibodies against DCAF7, TROAP and FAM117B were provided by Bethyl. Rabbit anti-Lamin (Cell Signaling, Cat# 2032S) and mouse Anti-Tubulin (Sigma, Cat# SAB1411818) antibodies were used to detect nuclear and cytoplasmic fractions, respectively, Mouse anti-Vinculin (Clone V9131, Sigma) was used as a loading control. Rabbit anti-GFP antibody (Cell Signaling, Cat# 29565) was used for immunoblotting. HRP conjugated anti-mouse IgG (Jackson lab, Cat# 115-035-003), HRP conjugated anti-rabbit IgG (Jackson lab, Cat# 111-035-003) and HRP conjugated anti-rabbit light chain IgG (Jackson lab, Cat# 211-032-171) were used as secondary antibodies for immunoblotting.

2.9 Cyto-Nuclear Fractionation

The established T98G cell lines were plated in p100 plates (1×10^6cells per plate) and allowed to attach overnight. The next day, the cells were scraped in PBS containing protease and phosphatase inhibitors and pelleted. Fresh pellets were first treated with hypotonic buffer in order to obtain the cytosolic extract and then with a hypertonic buffer in order to obtain the nuclear extract. A cytosolic and nuclear extraction kit was used for this purpose (Active Motif, Cat# 40010). Equivalent fractions (by volume) of the nucleus and cytoplasm were analyzed by western blotting.

2.10 Immunostaining and cell morphology experiment

For immunostaining, different T98G cell lines were plated on sterilized glass coverslips in 6-well plates (200,000 cells per well) and allowed to attach overnight. On the next day, the medium

from the wells was aspirated; the cells were washed with 1X PBS and then fixed by incubating with 2 mL 4 % paraformaldehyde (Ricca chemical company, Cat# 3191-31) for 30 min at RT. The cells were then washed with PBS, then permeabilized and blocked by incubating with 0.2 % Triton-X (Fisher Scientific, 9002-93-91) in 5% BSA for half an hour. The coverslips were incubated with the primary antibody (mouse anti-HA (Covance) diluted 1:100 in the blocking buffer) under humid conditions for 1 hour at RT. The coverslips were washed three times with PBS for 10 min each and incubated with the secondary antibody (Alexa Fluor 488 donkey anti-mouse IgG, Jackson lab) diluted 1:500 in the blocking buffer at RT for one hour. The coverslips were then washed as above, allowed to air dry, then mounted onto slides using mounting medium containing DAPI (Life Technologies, P36966) and sealed with clear nail polish. Images were captured using Zeiss Axio imager MAT reflected light microscope and 63X oil immersion lens.

For the actin staining experiment, cells were grown in 6-well plates, fixed as for immunostaining and permeabilized using 0.2% Triton X solution in PBS. The cells were washed thrice with PBS and incubated for half an hour in the dark with Actin Green 488 Ready Probes reagent (Life technologies) as suggested by the manufacturer and 0.1µg/mL DAPI in 1X PBS. The cells were washed with PBS and images were captured using Evos F1 microscope and 40X lens.

2.11 Transient transfections

Plasmids encoding GFP-tagged DYRK1A full length and deletions constructs were kindly provided by G. DeArcangelo (Yabut *et al*., 2010). The established T98G cell lines were transfected with the full length and deletion constructs using Mirus TransIT2020 reagent and OPTI-MEM according to the manufacturer's protocol using 300,000 cells and 1µg of DNA per

well of a 6-well plate. At 48 hours post transfection, the cells were lysed directly on the plate using EBC buffer with protease inhibitors, phosphatase inhibitors and βME and used for immunoprecipitation and Western blot analysis.

2.12 Cell proliferation assays

Cell proliferation was measured using crystal violet staining as described before (Litovchick *et. al*., 2011). For T98G parental and established CTAP and NTAP cell lines, the cells were counted and 3,500 cells per well were seeded in triplicates into two 12-well plates to be processed either on day 3 or day 5 post-plating. On day 3 or day 5, the cells were washed with 1X PBS and stained with Crystal Violet solution (Sigma, Cat# HT 90132). The plates were then rinsed by dipping into a beaker containing distilled water three to four times till there was no remaining residual dye, and allowed to air dry. The relative cell density was quantified by dissolving the dye in 10% (v/v) glacial acetic acid (ACROS, Cat# 64-19-7) in water and measuring the absorbance at 590nm, after which the ratio of cell density at day 5 to day 3 was calculated.

For U-2 OS cells, 50, 000 cells were plated per well of a 12 well plate, allowed to attach and then infected with VCMs to express the proteins of interest. The cells were subjected to puromycin selection 48 hours post infection. When the control (uninfected) cells were all dead (usually on day 3), the cells from each well were split into two plates such that all the cell lines were plated at similar densities. Each plate was designated to be processed on day 1 or day 5. The plates were stained with crystal violet dye and the results were quantified as described above. The cell density values obtained for the various cell lines were normalized to day 1.

The CTAP cell lines and NTAP cell lines were analyzed separately to determine the change in growth relative to the CTAP and NTAP GFP controls. An online two tailed t-test calculator for equal variances was used to determine if the differences in relative growth rates as compared to that of the controls were statistically significant.

For U-2 OS cells and U-2 OS DYRK1A null cells, a similar protocol as for T98G cell lines was followed. The cells were stained with crystal violet on day 1 and day 5 post plating and the cell density values relative to day 1 were compared.

CHAPTER 3: RESULTS

3.1 Generation of stable cell lines for characterizing DYRK1A-interacting proteins.

Most of the DYRK1A binding proteins have not been well characterized and some even have completely unknown functions. Since these proteins were identified through a large-scale proteomic analysis, it was important to independently verify these interactions through reciprocal immunoprecipitation experiments. However, since these proteins have not been extensively studied, the antibodies against most of them were not available at the start of the project. Moreover, the endogenous levels of these proteins were not known. Hence, we used the approach of retroviral infection to create stable cell lines expressing the desired proteins with an epitope tag. Since T98G human glioblastoma cell line was originally used for the DYRK1A's proteomic analysis, it was a reasonable choice for the confirmation of the interactions. Using retroviral infection of T98G cells followed by antibiotic selection, we generated a panel of seven cell lines expressing DYRK1A candidate interacting proteins fused with the dual FLAG-HA epitope tag (Figure 7 panel A). Western blot analysis using an HA antibody confirmed the

expression of the respective proteins in the obtained T98G cell lines. As shown in Figure 7B, all the HA-FLAG tagged proteins in the respective cell lines migrated on the SDS-PAGE according to their expected molecular weights. Although all the proteins were expressed using the same retroviral vector backbone, the levels of expression of the tagged proteins in the respective cell lines were found to be considerably different. This could be attributed to intrinsic differences in stability between the proteins in the panel.

An additional T98G cell line overexpressing LATS2 was also established along with this panel (data not shown) in order to exploit interaction of LATS2 with DYRK1A *in-vivo*, furthering the research by Tschop *et al.* (2011). However, characterization of this cell line needs further optimization and it was not included in our panel of DYRK1A-interacting proteins described in this thesis.

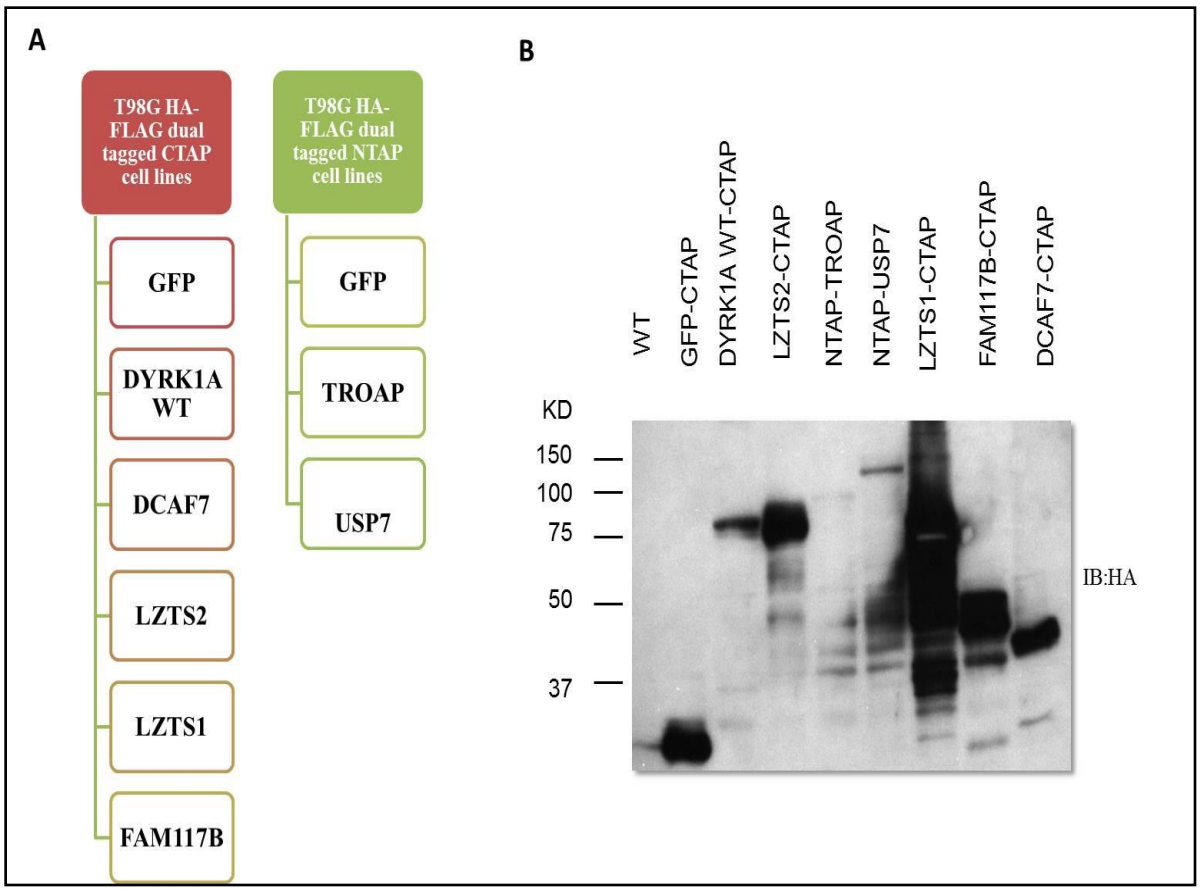

Figure 7: **T98G cell lines expressing the DYRK1A interacting proteins. A)** List of the T98G CTAP (C-terminal HA-Flag tag) and NTAP (N-terminal HA-FLAG tag) cell lines prepared for this study. **B)** Immunoblot showing the expression of the DYRK1A interacting proteins in the protein extracts prepared from the established T98G cell lines (equal amount of protein was loaded for all samples).

3.2 Confirming the interactions between DYRK1A and the candidate interacting proteins.

In order to confirm the interactions between DYRK1A and its candidate interacting partners, we performed a series of reciprocal immunoprecipitation-Western blotting experiments. After preparation of cell lysates, co-immunoprecipitations were performed with epitope-specific antibodies. Figure 8 gives a general overview of the steps involved. The proteins were first immunoprecipitated using an HA antibody and immunoblot analysis was carried out to detect DYRK1A in the immunoprecipitates. This interaction was then further verified by carrying out a

reciprocal pull down where DYRK1A was immunoprecipitated and the HA-tagged protein was detected in the immunoprecipitate. For cases where antibodies against the endogenous candidate proteins were available, endogenous pull down assays from T98G parental cells with these antibodies were also carried out followed by immunoblotting to detect DYRK1A in the immunoprecipitates.

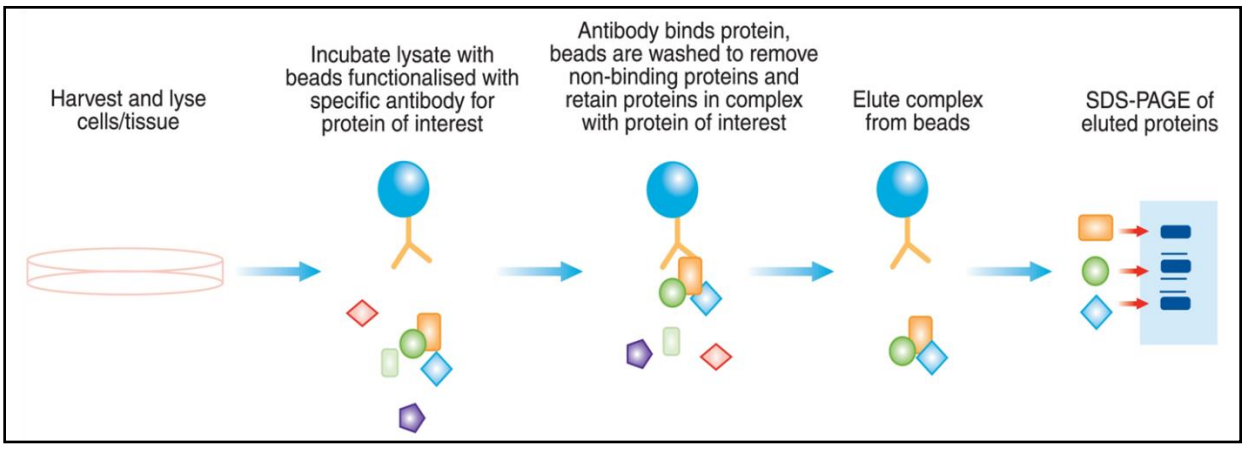

Figure 8: Schematic diagram showing the steps involved in immunoprecipitation analysis of interacting proteins (adopted from Proteome.org.au, n.d.).

MudPIT analysis of DYRK1A-interacting proteins revealed equal enrichment of DYRK1A and DCAF7, suggesting that these two proteins could interact stoichiometrically (L. Litovchick, unpublished data). Indeed, we observed a robust interaction between DYRK1A and DCAF7 both at the ectopically overexpressed and the endogenous levels (Figure 9). Since DCAF7 is a scaffold protein, it was interesting to determine if the DYRK1A interacting proteins also interacted with DCAF7.

The interactions between DYRK1A and LZTS1 or LZTS2 were confirmed through pull down with HA as well as pull down with DYRK1A (Figures 10 and 11 respectively). Interestingly,

both of these proteins interacted with DCAF7 as well. These interactions were also characterized at the endogenous level following characterization of a panel of rabbit polyclonal antibodies against LZTS1 and LZTS2 (data not shown) and used these antibodies to confirm the interaction with DYRK1A. Both these proteins also interacted with DCAF7.

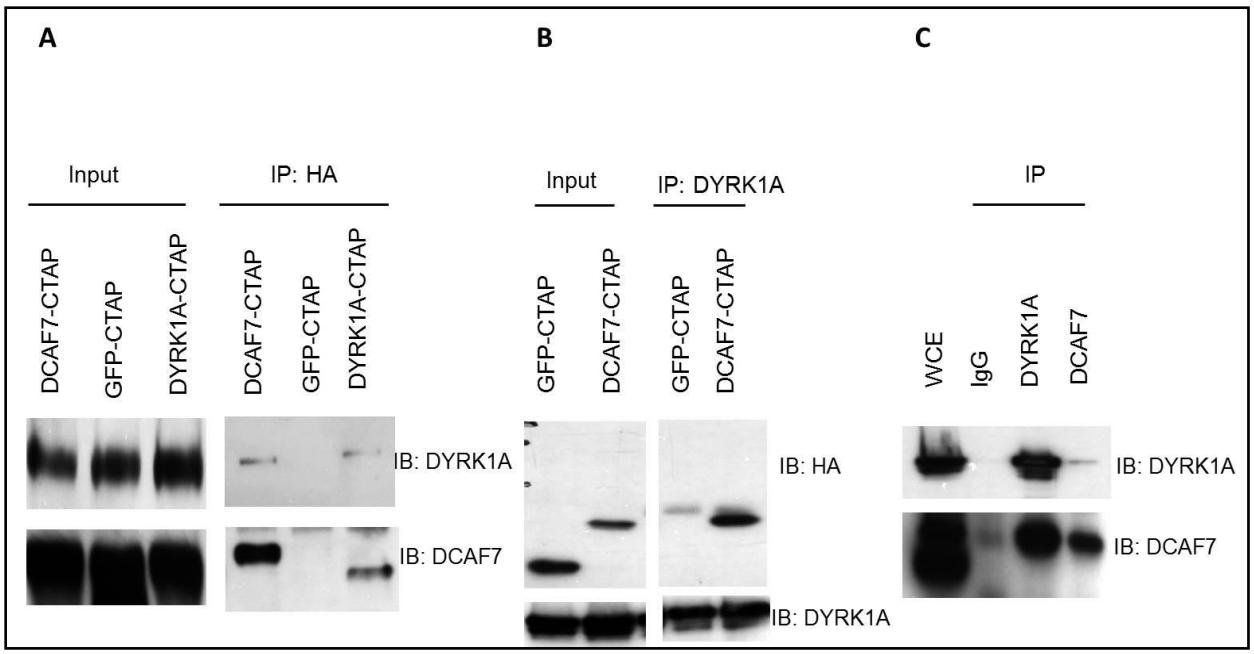

Figure 9: DYRK1A binds to DCAF7. Equal amounts of protein lysates were tested for protein expression (Input) or were used for immunoprecipitation experiments (IP) with the indicated antibodies. The eluted proteins were detected by immunoblotting (IB) as shown. A) The interactions were confirmed by immunoprecipitation with HA antibody and immunoblot analysis with DYRK1A and DCAF7 antibodies using T98G cell lines stably expressing the proteins of interest. The T98G-GFP cell line was used as a control. B) Reverse pull down was performed with anti-DYRK1A antibody followed by immunoblotting with HA antibody using T98G-GFP and T98G-DCAF7 cell lines. C) Confirmation of the interaction at the endogenous level was performed using T98G parental cells. IgG is a non-reactive antibody control. Whole cell extract (WCE) was used to detect protein expression.

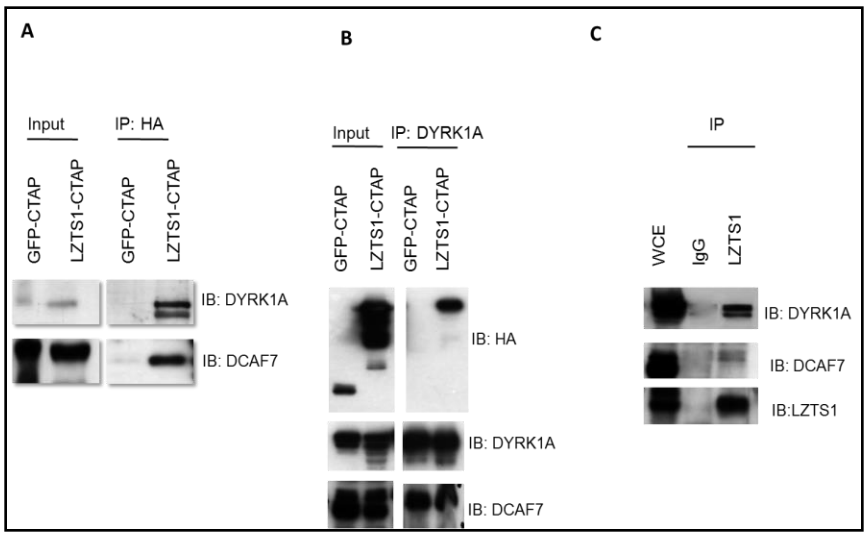

Figure 10: DYRK1A binds to LZTS1. A) The interactions were confirmed by immunoprecipitation with HA antibody and immunoblotting with DYRK1A and DCAF7 antibodies using T98G-LZTS1 cells. The T98G-GFP cell line was used as a control. B) Reverse pull down was performed with anti-DYRK1A antibody followed by immunoblotting with indicated antibodies. C) Confirmation of the interactions at the endogenous level was performed using T98G parental cells. IgG is a non-targeting antibody control. WCE, whole cell extract

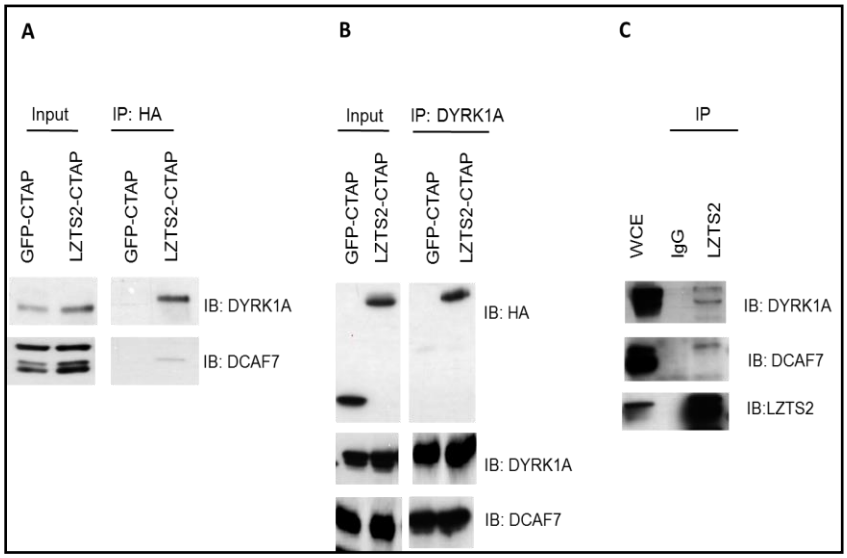

Figure 11: DYRK1A binds LZTS2. Experiments as in Fig. 10, only using T98G-LZTS2 cells.

Similarly, the DYRK1A's interactions with TROAP and FAM117B were also verified using pull down analysis with an HA antibody as well as with a DYRK1A antibody. We characterized a panel of rabbit polyclonal antibodies against TROAP and FAM117B (data not shown) and used

these antibodies to confirm the interaction with DYRK1A at the endogenous level. Remarkably, both these proteins interacted with DCAF7 (Figure 12 and 13), raising a possibility that DCAF7 DCAF7 could mediate the interaction between DYRK1A and other proteins.

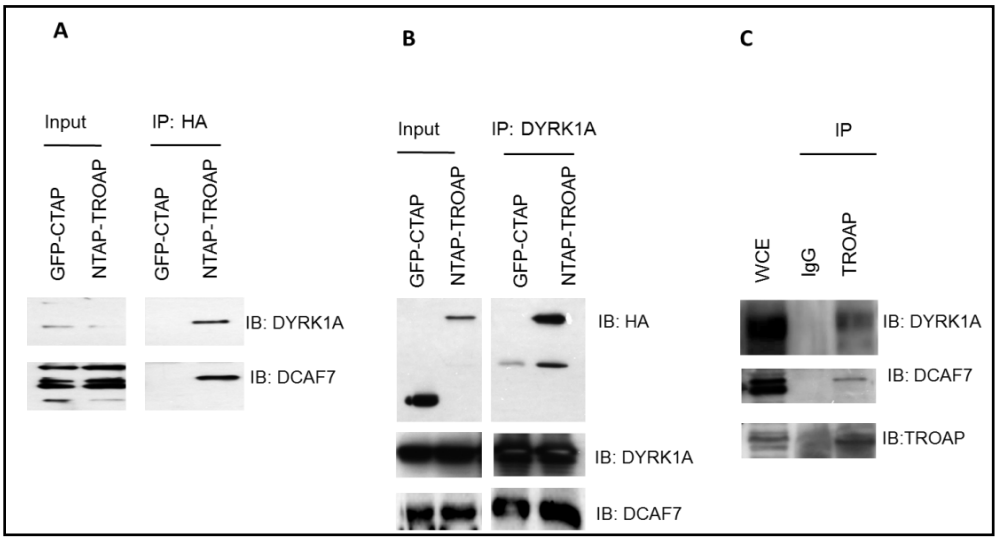

Figure 12: DYRK1A binds TROAP: A) The interactions were confirmed by immunoprecipitation with HA antibody and immunoblotting with DYRK1A and DCAF7 antibodies using T98G-TROAP cells. The T98G-GFP cell line was used as a control. B) Reverse pull down was performed with anti-DYRK1A antibody followed by immunoblotting with indicated antibodies. C) Confirmation of the interactions at the endogenous level was performed using T98G parental cells. IgG is a non-targeting antibody control. WCE, whole cell extract

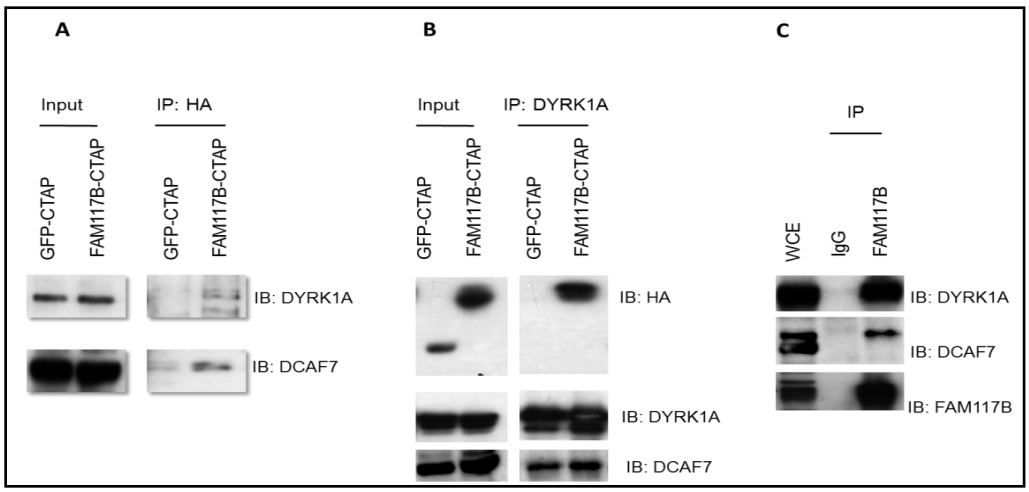

Figure 13: DYRK1A binds FAM117B. Experiments as in Figure 12, only using T98G-FAM117B cell line and anti-FAM117B antibodies.

We also carried out validation of the interactions between DYRK1A and two other proteins detected by MudPIT, USP7 and RNF169. We were not able to detect co-immunoprecipitation between DYRK1A and USP7 in the extracts prepared from T98G-USP7 stable cell line (data not shown). However, a weak interaction between these proteins was detected using transient co-expression of DYRK1A and USP7 in T98G cells (data not shown). It is possible that DYRK1A and USP7 interact only under certain conditions and further studies will be required to characterize this interaction. The interaction of DYRK1A with RNF169 has been confirmed using transient transfections and endogenous binding studies (V. Menon and L. Litovchick, unpublished data). Interestingly, the interaction between RNF169 and USP7 was also detected, suggesting that DYRK1A could be involved into multi-subunit protein complexes (data not shown).

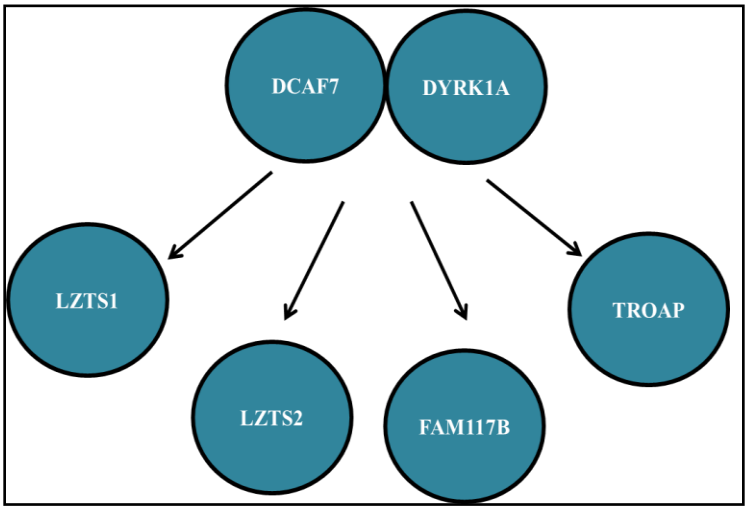

Figure 14: A graphical representation of the DYRK1A interactions confirmed by immunoprecipitation-Western blotting. Notably, all these DYRK1A binding proteins also interact with DCAF7.

3.3 DYRK1A interacting proteins are localized both in the cytoplasm and in the nucleus.

While DYRK1A is found both in the nucleus and the cytoplasm, localization of most of the DYRK1A interacting proteins is not known. Binding of DYRK1A to DCAF7 induces nuclear localization of the predominantly cytosolic protein DCAF7 (Miyata Y., 2011), suggesting that DYRK1A could have a role in regulating cellular localization of its interacting proteins. Therefore, we looked at the localization of these proteins through cyto-nuclear fractionation and immunostaining using a panel of stable T98G lines described above.

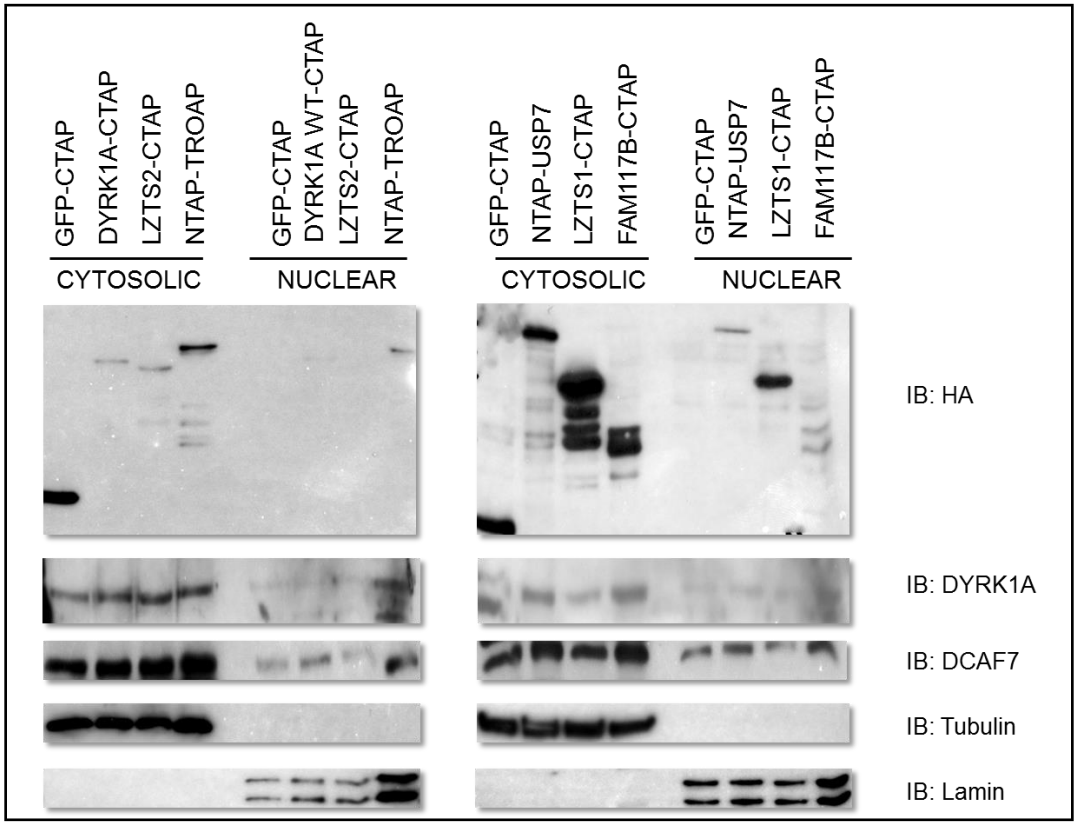

Figure 15: Nucleo-cytoplasmic distribution of the DYRK1A interacting proteins. The T98G cell lines expressing the indicated proteins were fractionated to obtain cytoplasmic and nuclear extracts. Equal fractions of each cytoplasmic and nuclear sample (cell equivalents) were analyzed by Western blotting using an anti-HA antibody as well as antibodies against DYRK1A and DCAF7. Tubulin and lamin serve as markers for cytosolic and the nuclear fractions, respectively.

The cyto-nuclear fractionation analysis revealed that most of the DYRK1A interacting proteins are enriched in the cytoplasm (Figure 15). In order to test if overexpression of these DYRK1A interacting proteins could affect the nucleo-cytoplasmic distribution of the endogenous DYRK1A and DCAF7, we analyzed the levels of DYRK1A and DCAF7 in these compartments of the various cell lines. As shown in Figure 15, there were no major differences in the levels of DYRK1A or DCAF7 in different cell lines.

In order to obtain a deeper insight into localization of DYRK1A-interacting proteins, we performed indirect immunofluorescence cell staining of the established T98G cell lines using anti-HA antibody. HA-tagged LZTS2, DYRK1A and FAM117B showed a pan cellular distribution while HA-tagged DCAF7 and TROAP appeared to be predominantly cytosolic and excluded from the nucleus (Figure 16). Interestingly, it was also observed that HA-DYRK1A was enriched in the nuclei of at least some of the cells (Figure 16). HA-tagged USP7 and HA-tagged LZTS1 appeared to be mainly nuclear proteins.

A

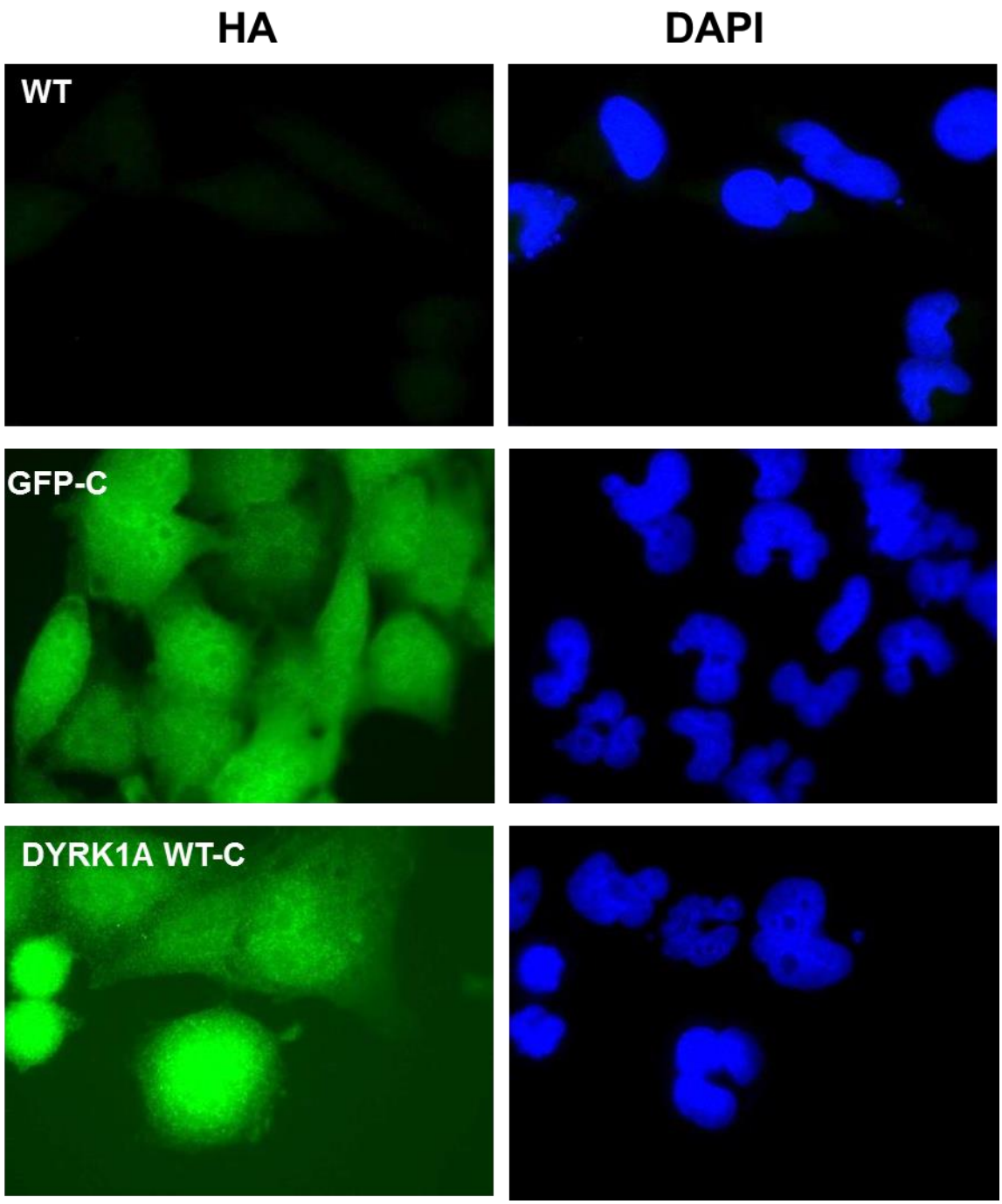

B

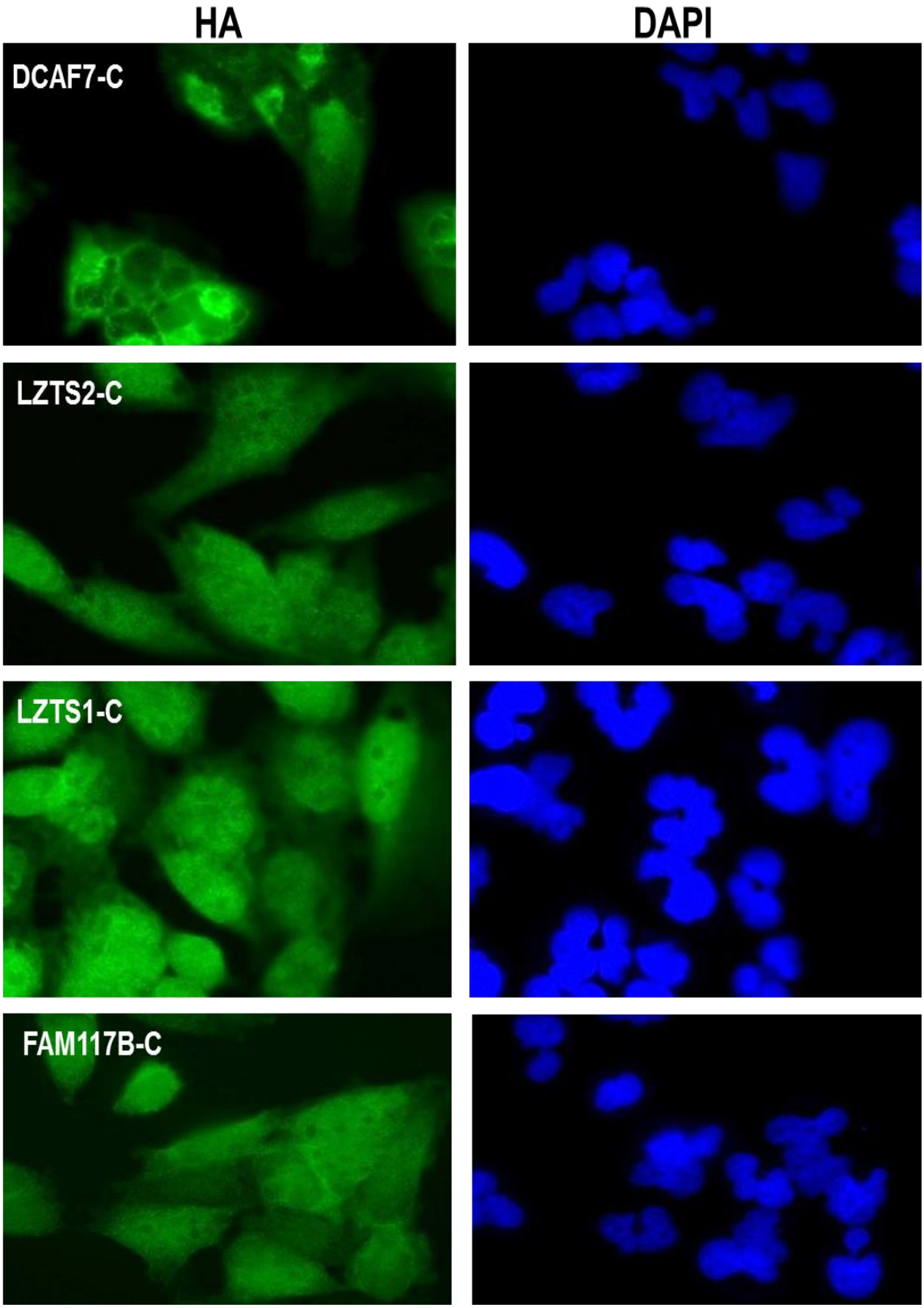

C

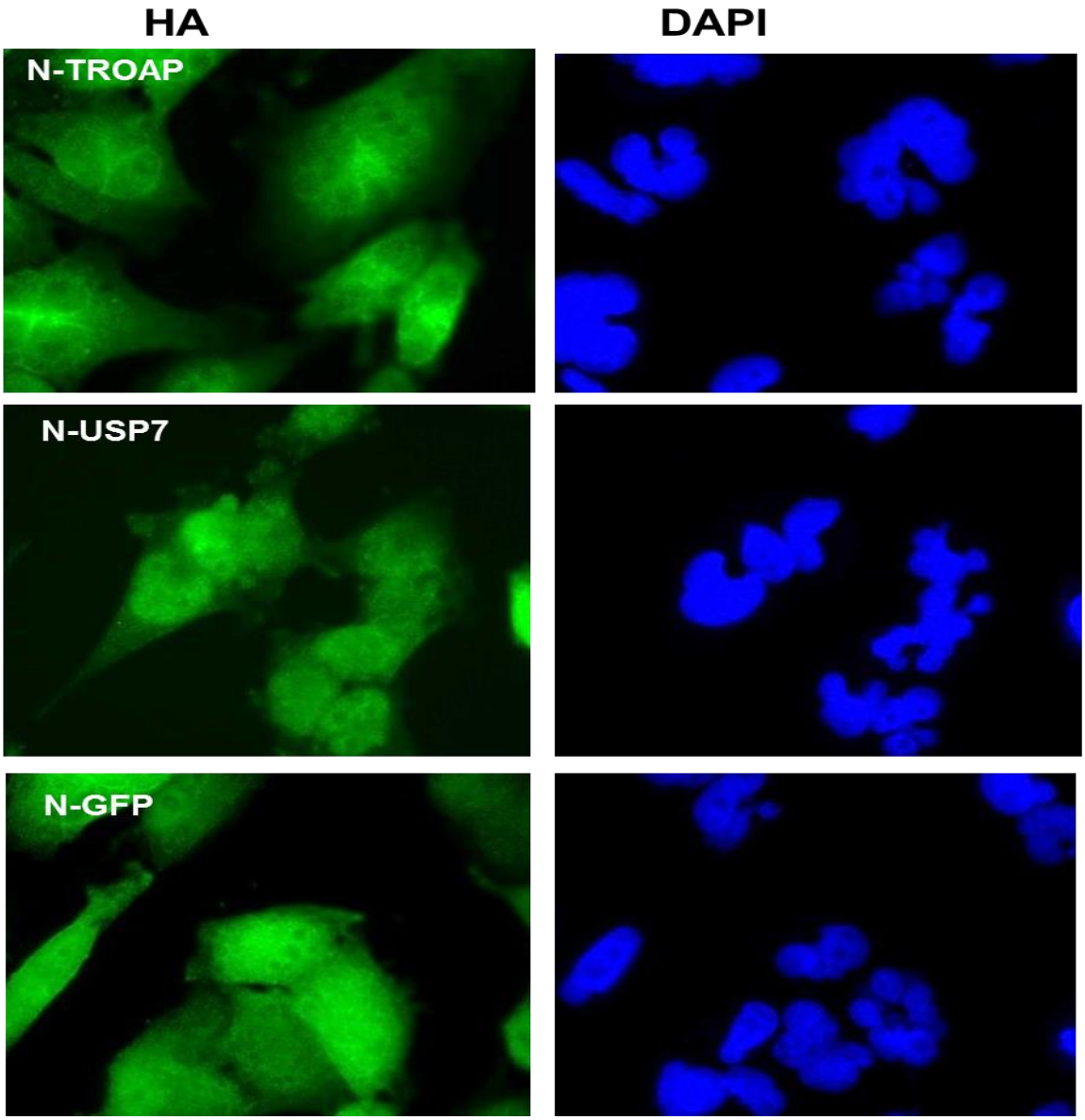

Figure 16: DYRK1A interacting proteins are localized in different cellular compartments. The indicated T98G cell lines were grown on glass coverslips, fixated, stained with anti-HA antibody and DAPI (to detect the nuclei). The images of representative cells at 63x magnification are shown in panel A, B and C. The parental T98G cell line (WT) was used as a control for HA staining.

3.4 DCAF7 could mediate the DYRK1A binding to LZTS1, LZTS2 and FAM117B.

It has been previously reported that The N-terminal region of DYRK1A is essential for its binding to DCAF7 (Miyata, 2011). We wished to confirm this report by mapping the region required for the binding of DCAF7 to DYRK1A. T98G-DCAF7 cells were transiently transfected with GFP-tagged deletion constructs of DYRK1A (Figure 17) followed by immunoprecipitation with HA antibody and analysis of the immunoprecipitate for the presence of GFP. In agreement with the previous report, we found that the DYRK1A-GFP construct in which the first 102 amino acids were deleted did not bind the HA-tagged DCAF7 (Figure 18). Interestingly, the deletion or mutation of the kinase domain of DYRK1A had no effect on its binding to DCAF7 (Figure 18).

Since our data suggest that DCAF7 interacts with a number of DYRK1A-binding proteins, we hypothesized that it could mediate the binding between these proteins and DYRK1A. Since we established that the Δ1-102 mutant of DYRK1A does not bind DCAF7, we wished to analyze if this fragment can bind to other DYRK1A interacting proteins. To do so, T98G cell lines expressing LZTS1, LZTS2 or FAM117B were transiently transfected with the Δ1-102-DYRK1A-GFP and used for anti-HA IP followed by anti-GFP immunoblotting. It was found that HA-tagged LZTS2, LZTS1 and FAM117B could not bind the Δ 1-102 mutant of DYRK1A that is unable to interact with DCAF7 (Figure 19). Therefore DCAF7 could mediate the interactions between DYRK1A and these proteins. Alternatively, it is also possible that DCAF7, LZTS1, LZTS2 and FAM117B all bind to the N-terminal region of DYRK1A. It will be important to establish in the future if the 1-102 a.a. N-terminal fragment of DYRK1A is sufficient for binding to DCAF7 or other DYRK1A–interacting proteins in question. It would be also interesting to

determine whether LZTS1/2 and FAM117B can be a part of the same protein complex with DYRK1A and DCAF7.

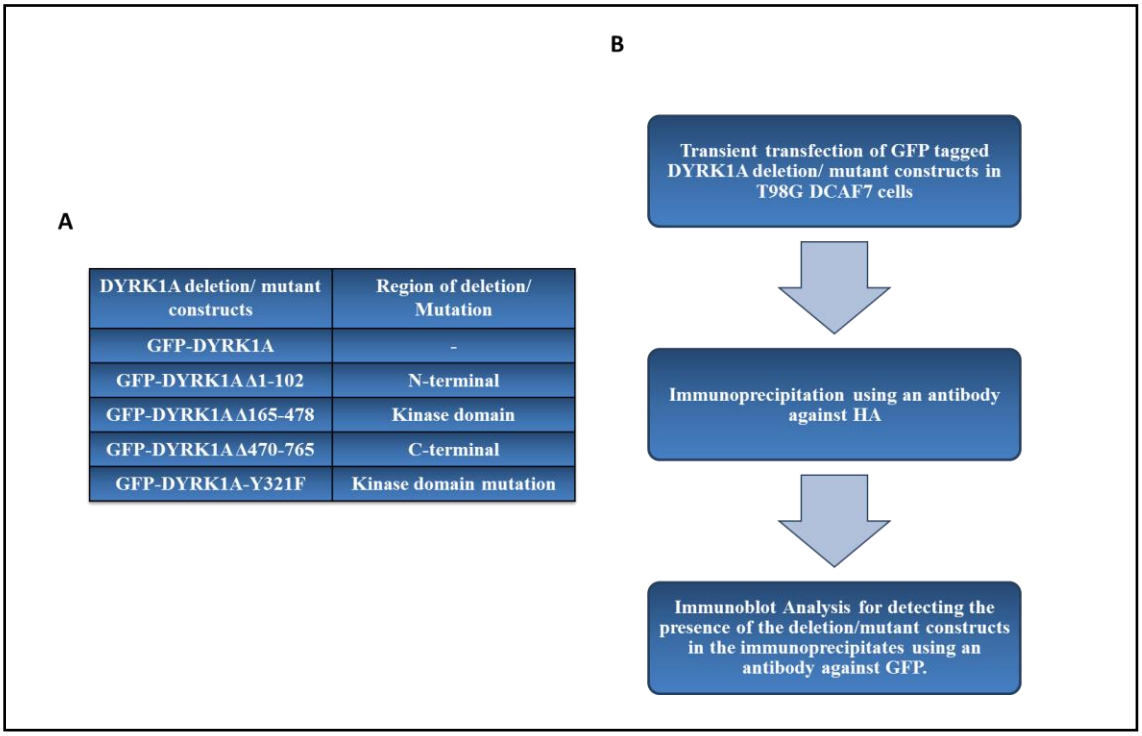

Figure 17: Method to map the DCAF7-bindning domain in DYRK1A. Panel A) Table shows the DYRK1A constructs used for transient transfection. Panel B) Design of the experiment.

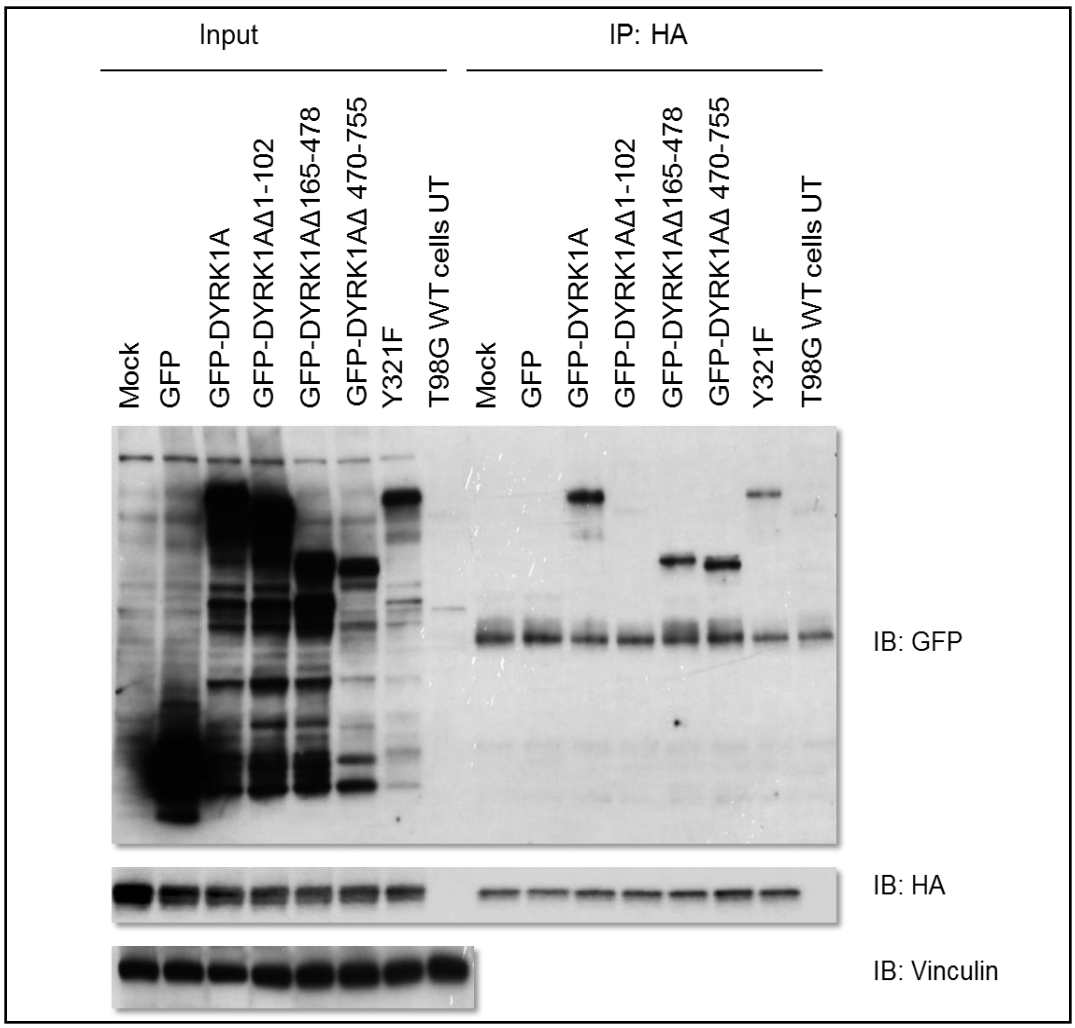

Figure 18: First 102 amino acids of DYRK1A are required for DCAF7 binding. T98G-DCAF7 cells were transfected and processed as in Fig. 18. T98G parental cells and untransfected T98G-DCAF7 (mock) cells were used as controls. Equal amounts of protein lysates were tested for protein expression (Input) using Vinculin as a loading control.

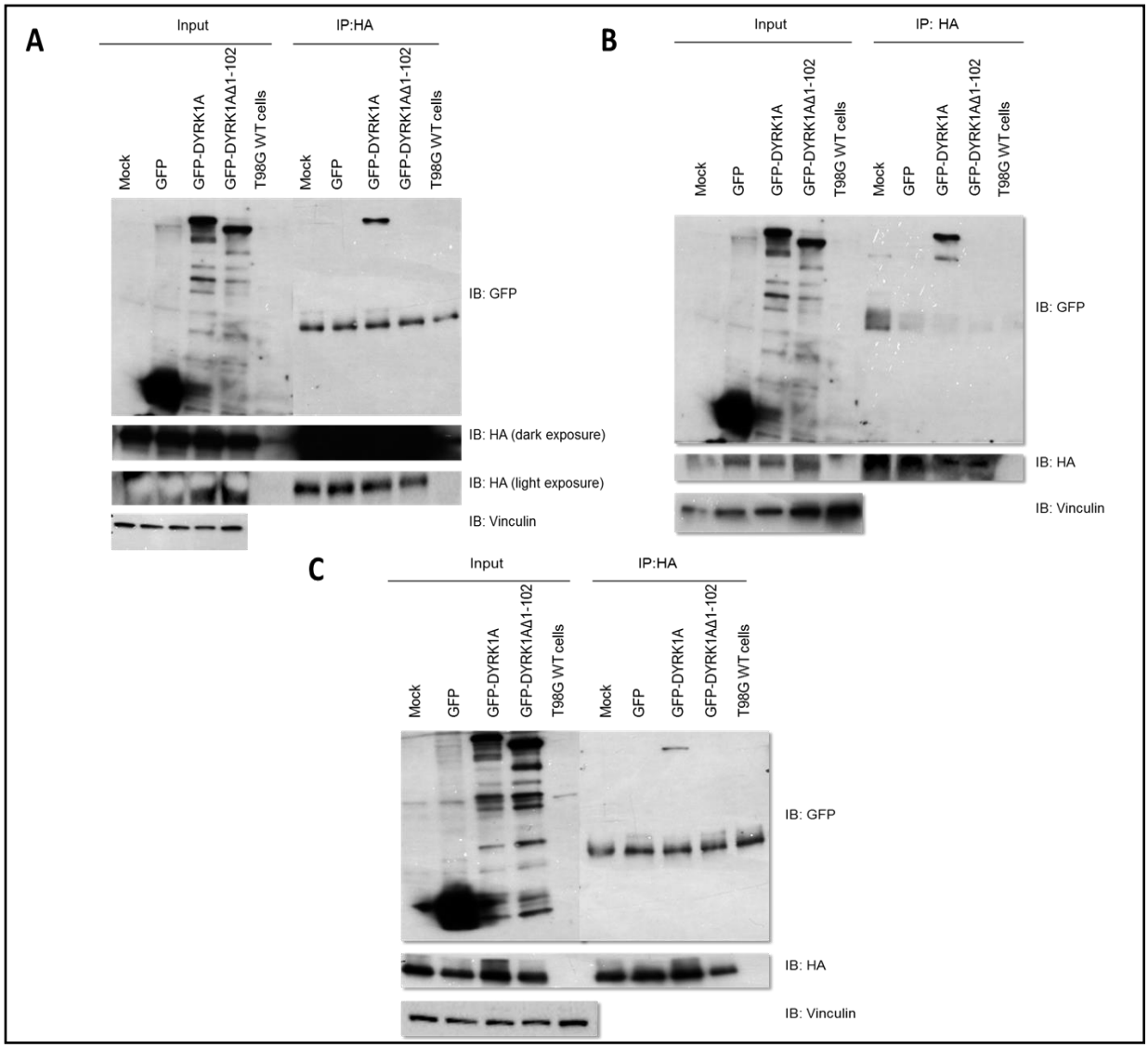

Figure 19: The first 102 amino acids of DYRK1A are necessary for its binding with LZTS2, LZTS1 and FAM117B. A) T98G-LZTS1, B) T98G LZTS2 and C) T98G FAM117B cells were transiently transfected with either wild type or the Δ1-102 deletion mutant DYRK1A. The immunoprecipitation of the HA tagged proteins was confirmed by immunoblotting with anti-HA antibody. T98G parental cell lines and the corresponding untransfected (mock) cell lines were used as controls. Equal amounts of protein lysates were tested for protein expression (Input) using Vinculin as a loading control.

3.5 The effect of the validated DYRK1A-interacting proteins on the T98G cell proliferation.

DYRK1A has been shown to inhibit cell proliferation when overexpressed in various human cancer cell lines (Litovchick *et al*. 2011). There is also evidence that DCAF7 could be required

for cellular proliferation (Miyata, 2011 and Ritterhoff, *et al*. 2010). Therefore, we were interested to determine whether DYRK1A interacting proteins could regulate cellular proliferation. We compared proliferation of T98G stable cell lines expressing DYRK1A, its interacting proteins or control cells using crystal violet staining assay. As shown in Figure 20, expression of DYRK1A, LZTS2, DCAF7 or USP7 significantly affected T98G cell proliferation.

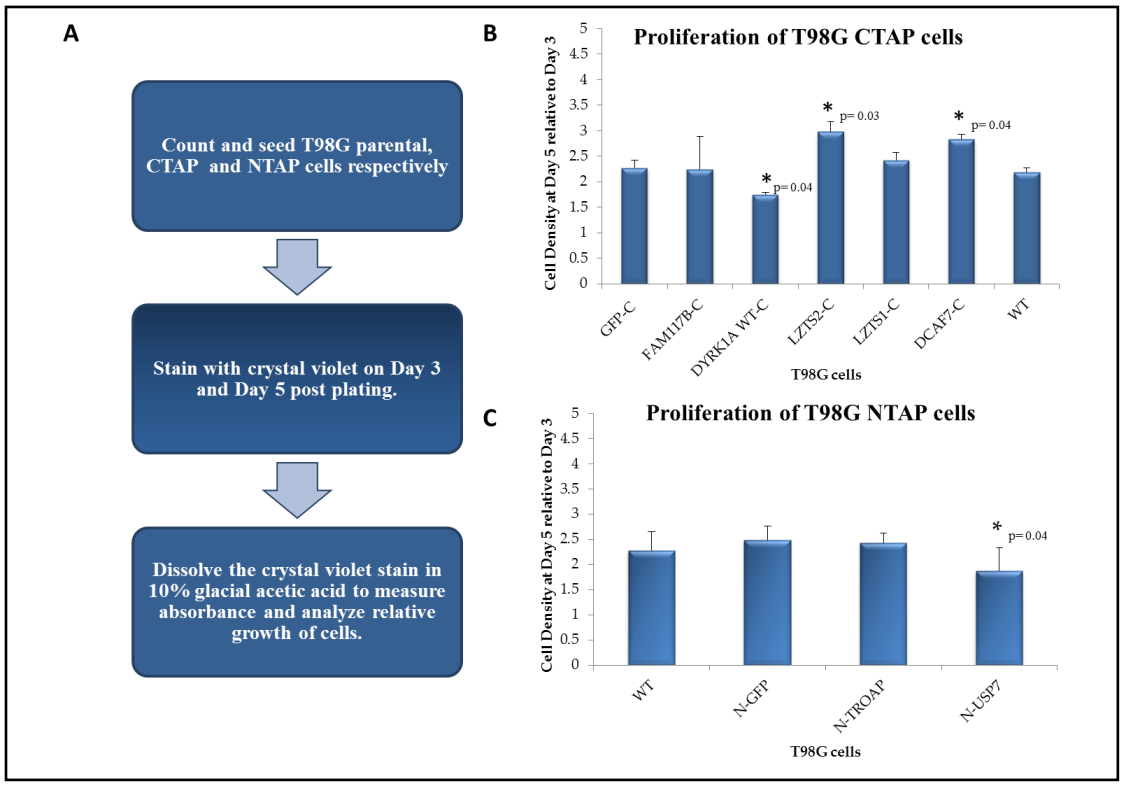

Figure 20: The effect of DYRK1A interacting proteins on the proliferation of T98G cells. A) Design of the experiment. B) Proliferation of T98G CTAP cell lines as measured by increase of the cell density on day 5 relative to day 3. Graph shows average values +/- standard deviation of two independent experiments each performed in triplicate. Untreated T98G and T98G GFP CTAP cell lines were used as controls. C) Same as B, only with T98G NTAP cell lines. Student's two-tailed t-test was performed for the statistical analysis in which the CTAP- and NTAP- cell lines were compared to their respective GFP controls.

3.6 The role of DYRK1A and its interacting proteins in regulation of actin cytoskeleton.

The study published by Park *et. al*., suggested that DYRK1A could be involved in the regulation of the actin cytoskeleton (Park et. al., 2011). The T98G cells overexpressing various DYRK1A

interacting proteins appeared to have distinct cellular morphologies that could be mediated by changes in their cytoskeleton. We used fluorescent labeled phallotoxin derivative (Actin Green 488 Ready Probe, Life Technologies) to stain actin filaments in a panel of stable T98G cell lines described above. DYRK1A overexpression in T98G cells shows an increase in the number and prominence of the actin stress fibers in the cell, resulting in a denser and more bright actin staining while DCAF7-overexpressing cells have a similar phenotype (Figure 21). Both LZTS1- and LZTS2-overexpressing cells appear to have an increased number of the short filopodia-like protrusion from several edges of the cell while the density of stress fibers seems to be decreased (Figure 21). We also observed and increased accumulation of actin in the nucleus in the FAM117B-overexpressing cells as compared to the parental cell control. The overexpression of USP7 and TROAP does not seem to cause distinct changes in the actin pattern (Figure 21).

A

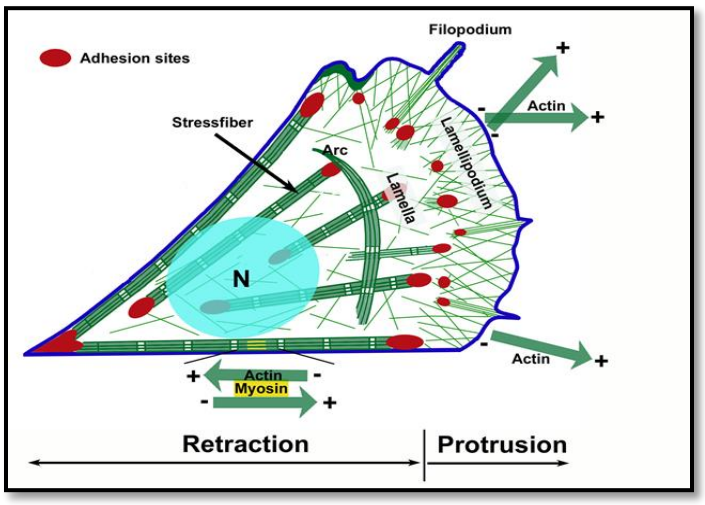

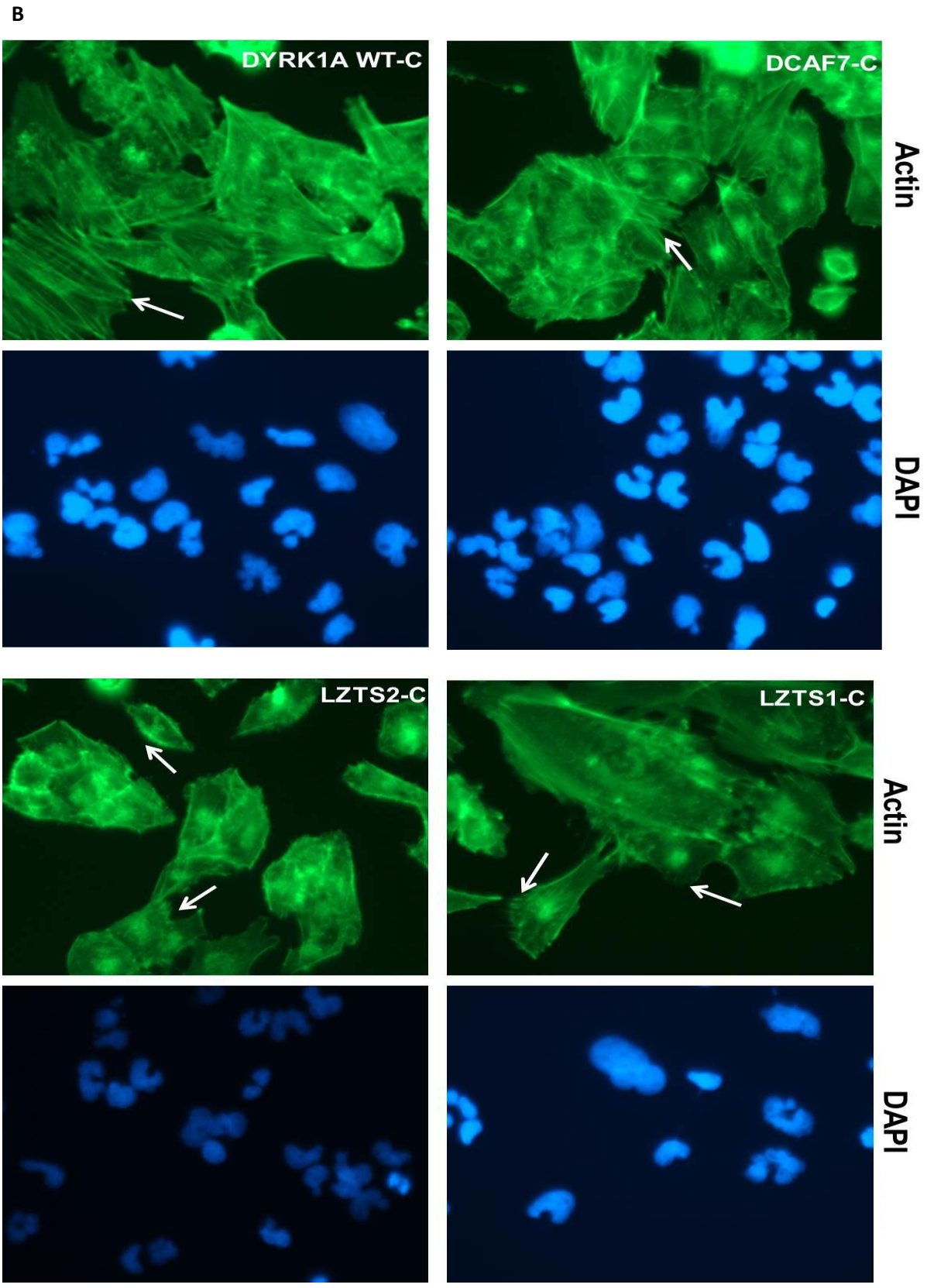

Figure 21: The effect of DYRK1A and its interacting proteins on actin cytoskeleton.

C

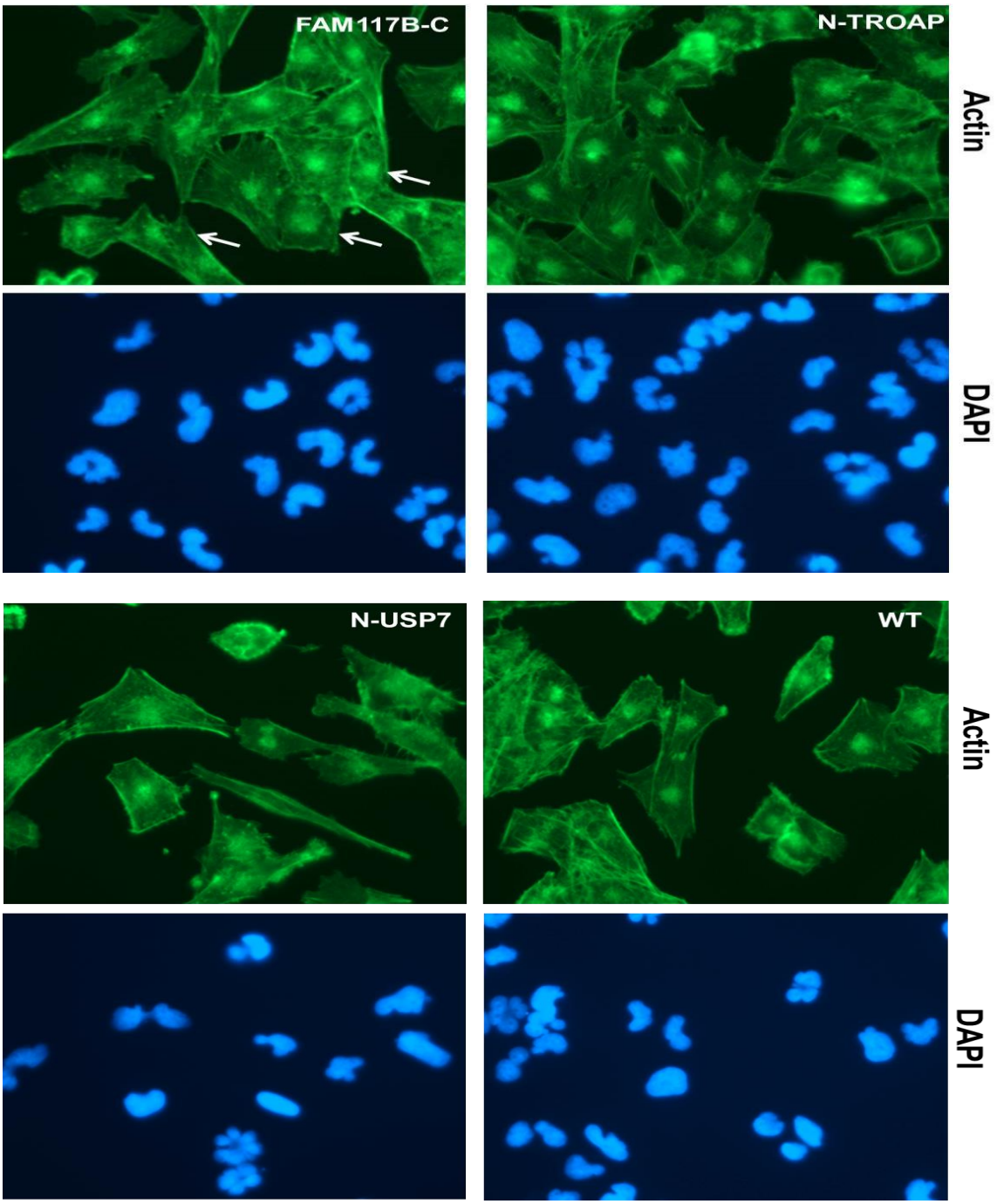

Figure 21: The effect of DYRK1A and its interacting proteins on actin cytoskeleton. Panel A shows a schematic presentation of different cytoskeletal structures (open access image, Google images). B and C) The T98G cell lines cells were fixed, permeabilized and stained with fluorescent dyes to detect actin (green) or DNA (DAPI, blue). Representative images taken at 40X magnification are shown. White arrows indicate the distinct actin patterns observed.

3.7 Generation of additional cell-based models for characterization of DYRK1A-interacting proteins.

The overexpression of DYRK1A variably inhibits proliferation of most cancer cell lines but it causes a potent growth arrest in U-2 OS cells (Litovchick *et. al*., 2011). This increased sensitivity of U-2 OS cells could be due to a genetic loss of one allele of *DYRK1A* (L. Litovchick, unpublished data). Therefore, we sought to determine the effect of overexpression of DYRK1A interacting proteins in these cells. This could give us an insight about the proteins that could act in conjunction with DYRK1A to promote its function of causing cell cycle arrest or about the proteins that oppose the growth arrest function of DYRK1A. Since stable cell line to express DYRK1A in U-2 OS cells could not be established, we used a transient retrovirus-mediated expression of the DYRK1A-interacting proteins in these cells (Figure 22).

In agreement with previous findings, overexpression of DYRK1A showed a potent trend of suppression of proliferation in U-2 OS cells (Figure 22). Remarkably, a similar suppression of cellular proliferation was also observed upon overexpression of USP7 in U-2 OS cells (Figure 22). These effects were statistically significant with p-values of 0.00013 for DYRK1A and 0.05 for USP7. Therefore, it is possible that USP7 could act in conjunction with DYRK1A to suppress cellular proliferation in this cell type. On the other hand, overexpression of DCAF7, FAM117B and TROAP showed a trend of increasing cellular proliferation when compared to the control GFP-expressing cells although these effects did not achieve a statistical significance (Figure 22).

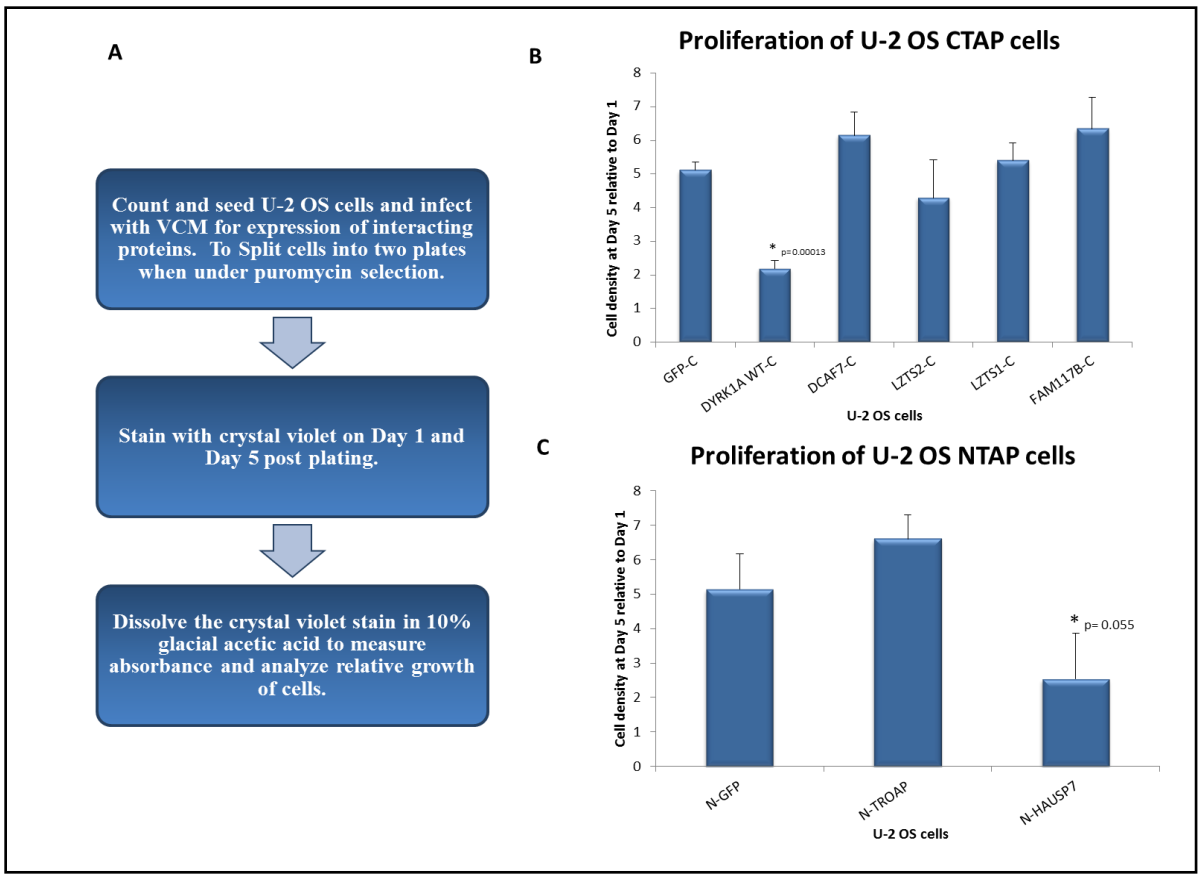

Figure 22: The effect of DYRK1A interacting proteins on the proliferation of U-2 OS cells. A) A flow chart of the procedure followed for the cellular proliferation assay in U-2 OS cells. B) Proliferation of U-2 OS CTAP cell lines as measured by increase of the cell density on day5 relative to day 1. The graph shows average values +/- standard deviation of three independent experiments. The U-2 OS GFP CTAP cell line was used as a control. C) Same as B, only with U-2 OS NTAP cell lines. Student's two-tailed t-test was performed for the statistical analysis in which the CTAP- and NTAP- cell lines were compared to their respective GFP controls.

In order to further characterize the function of the DYRK1A-interacting proteins, the DYRK1A-null U-2 OS cell lines were generated in our laboratory using the CRISPR-Cas9 technology (S. Saini and L. Litovchick, unpublished data). For initial characterization of these cells, we performed a cell proliferation assay using crystal violet staining. Unexpectedly, the U-2 OS-DYRK1A-null showed a markedly decreased cell proliferation when compared to U-2 OS parental cells (Figure 23B). This result was significant with a p-value of 0.002. This suggests that

DYRK1A plays an essential role in cell proliferation and both increase and decrease of the DYRK1A levels results in reduced proliferation rates.

Furthermore, we also generated a rescue cell line in which DYRK1A was stably re-expressed in the U-2 OS-DYRK1A-null cells (Figure 24, courtesy of Dr. V. Menon, Litovchick lab). This set of U-2 OS cell lines will serve as useful tool for the future experiments on characterizing the DYRK1A-interacting proteins as well as understanding DYRK1A-regulated pathways in the cells using gene expression analysis, proteomics and functional assays.

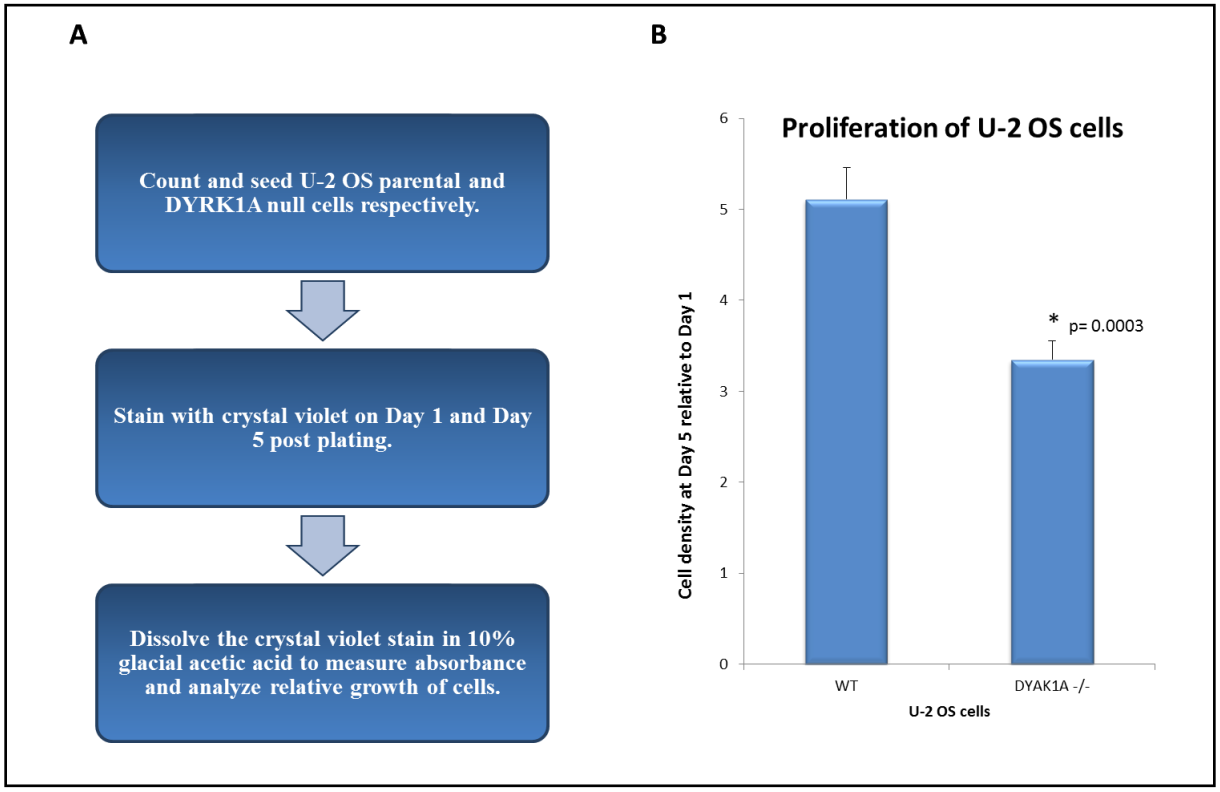

Figure 23: Loss of DYRK1A inhibits cell proliferation of U-2 OS cells. A) A flowchart of the procedure followed for the experiment. B) Cell proliferation assay comparing the U-2 OS WT (DYRK1A +/-) and U-2 OS-DYRK1A-null cells (-/-). The graph shows average of four biological replicates. The two tailed Student's t- test was used for the statistical analysis.

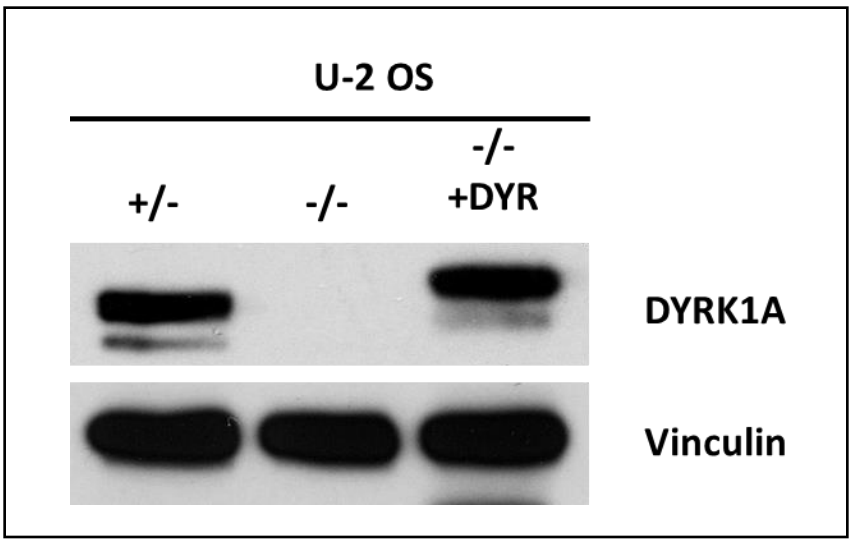

Figure 24: Expression of DYRK1A in the U-2 0S cell models. U-2 $OS^{+/-}$ indicates the wild type cell line (haploid for *DYRK1A*). U-2 $OS^{-/-}$ indicates the null cells and U-2 $OS^{-/-}$ +DYR indicates the null cells in which DYRK1A has been reintroduced. Vinculin is shown as a loading control

CHAPTER 4: DISCUSSION

4.1 DYRK1A interacts with a diverse group of cellular proteins.

In this study, we confirmed the interaction between DYRK1A and seven candidate interacting proteins previously detected by mass-spec proteomic analysis. Since the data on their function and even cellular localization was limited, we performed initial characterization of these factors and their effect on regulation of cell proliferation and actin cytoskeleton, the functions previously attributed to DYRK1A. Our immunostaining experiments using T98G cell lines over expressing DYRK1A interacting proteins revealed distinct localizations of some of the proteins, suggesting that DYRK1A could play different roles in specific cellular compartments. Previous evidence shows that DYRK1A promotes nuclear localization of the predominantly cytosolic protein DCAF7 (Miyata., 2011), suggesting that DYRK1A could have a role in localization of its interacting proteins. It will be interesting to determine in the future studies if the overexpression or depletion of DYRK1A can affect the cellular localization of its interacting proteins. Similarly, the interacting proteins could be involved in the distribution of DYRK1A between the different compartments in the cell or mediate distinct DYRK1A functions at these compartments.

Our initial characterization of the role of the DYRK1A-interacting proteins in cell proliferation also revealed diverse effects. Cell proliferation experiments in both T98G and U2-OS cells revealed that USP7 has a similar growth inhibitory function to DYRK1A. It is possible that USP7 contributes to the growth suppressive function of DYRK1A as an upstream activator or a downstream effector. USP7 is a deubiquitinating enzyme that removes ubiquitin moieties from target proteins such as p53 and MDM2 (Vogelstein et al., 2000) as well as other factors with relevance to apoptotic cell death pathways. Our study did not discriminate between inhibition of cell proliferation and cell death and it will be important to further compare the mechanisms of the USP7 and DYRK1A-mediated growth suppression in the future. We also observed that some of the DYRK1A-interacting proteins such as DCAF7, FAM117B and TROAP appeared to increase the cell proliferation. These factors could be involved in antagonizing the growth suppressor function of DYRK1A and it will be important to determine if these effects could promote tumorigenesis. Finally, even though increased expression of DYRK1A results in potent growth suppression in U-2 OS cells, we found that complete genetic loss of DYRK1A in these cells also results in reduced proliferation. This result indicates that DYRK1A is essential for optimal progress through the cell cycle or for the cell survival. It will be interesting to determine the cell cycle profiles of these cells for better understanding of the mechanisms of this phenomenon.

We also observed a variation of effects of the DYRK1A-interacting proteins on actin cytoskeleton. In particular, we observed an apparent increase in the number and prominence of actin stress fibers in T98G cell lines overexpressing DYRK1A or DCAF7. Stress fiber formation is under control of the RhoA GTPase signaling pathway (Figure 25) where RhoA-mediated

activation of mDia1 at the plasma membrane is responsible for the actin-nucleating activity required for stress fiber formation (Pellegrin and Mellor, 2007; Figure 25). RhoA also activates myosin contractility through activation of ROCK and PKN kinases (Fig. 25). Intriguingly, DCAF7 (HAN11) has been shown to bind mDia1 and mDia2 (Morita *et al*., 2006). Furthermore, mDia and active RhoA increase the cytoplasmic retention of DCAF7 while expression of the dominant-negative RhoA promotes nuclear localization of DCAF7. DCAF7 and active form of mDia both inhibited DYRK1A's ability to activate GLI1-mediated transcription, resulting in suppression of the Hedgehog signaling (Morita *et al*., 2006). It will be interesting to determine whether DCAF7 and the RhoA signaling can regulate other functions of DYRK1A in the nucleus including the regulation of the DREAM repressor complex and to determine the role of DYRK1A-DCAF7 complex in the activation of RhoA signaling.

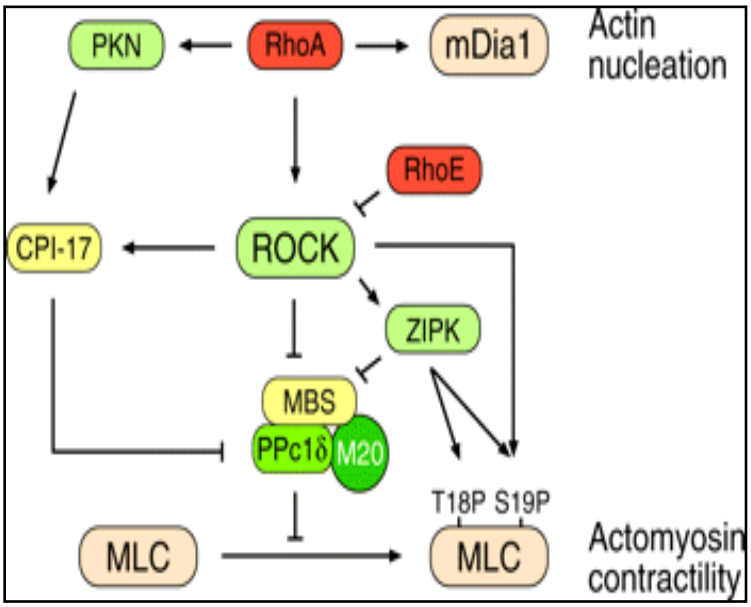

Figure 25: Signaling pathways controlling stress fiber formation (Adopted from Pellegrin and Mellor, 2007).

4.2 The role of DCAF7 as a major DYRK1A-interacting protein

Our results demonstrate that DCAF7 binds all DYRK1A interacting proteins validated in this study. Furthermore, our results also suggest that blocking the DCAF7 binding by N-terminal deletion prevents the binding of other interacting proteins to DYRK1A mutant. Importantly, DCAF7 has five WD40 repeat domains (Miyata *et al.*, 2011) that could facilitate protein-protein interactions (Smith *et al*., 1999; Li and Roberts, 2001). Scaffolding function of DCAF7 has been previously proposed with respect to HIPK2 and MEKK1 kinase functions **(**Ritterhoff *et al*., 2010)**.** Our finding that DCAF7 could be required for the interactions of the other proteins with DYRK1A needs to be confirmed using siRNA knockdown of DCAF7. The apparent opposite effects of DYRK1A and DCAF7 on cell proliferation make it interesting to determine whether DCAF7 contributes to a particular function of DYRK1A in a specific cellular compartment.

We found that four of the DYRK1A interacting proteins (DCAF7, LZTS1, LZTS2 and FAM117B) require the first 102 amino acids of DYRK1A in order to bind. Interestingly, this region is very close to the nuclear localization signal of DYRK1A located between 105 and 139 amino acids and could be responsible for DYRK1A's localization in nuclear sub-compartments (Becker *et. al*., 1998). Most of the DYRK1A interacting proteins are present in the nucleus and it will be interesting to characterize their interaction with DYRK1A in cytoplasmic and nuclear fractions. Additionally, it will be important to determine whether the first 102 amino acids of DYRK1A are required for the kinase activity of DYRK1A towards LIN52, for its ability to promote DREAM assembly and to induce growth arrest in U-2 OS cells.

4.3 DYRK1A and TROAP

Interaction between DYRK1A and TROAP could reveal a new mechanism for understanding of the Down syndrome pathogenesis. There is evidence that DYRK1A can contribute to phosphorylation of the human microtubule-associated protein Tau at 11 known sites. These sites are significantly hyper phosphorylated in the DS brain, leading to the reduction of the biological function of Tau due to increased self- aggregation and fibrillization, ultimately causing neuronal death. The microtubule assembly is also compromised (Liu *et. al*., 2007 and 2008; Wegiel *et. al*., 2011), possibly contributing to dendritic shortening and atrophy in DS (Tejedor and Hammerle, 2010). However, it is not known how DYRK1A is recruited to microtubules and regulates Tau. Since TROAP is thought to be associated with microtubules (Nadano *et. al*., 2002), it will be interesting to determine if TROAP contributes to the activity of DYRK1A associated with microtubules. If it does play a role, TROAP could be targeted to alleviate the symptoms of DS.

Understanding the roles of the DYRK1A interacting proteins and molecular mechanisms of their interaction with DYRK1A could improve our understanding of the DYRK1A function and regulation. Our data show that cellular phenotypes are strongly influenced both by increased and decreased DYRK1A levels suggesting that further studies are required to understand the phenotypes observed due to the genetic gains (i.e., DS) or losses (i.e., cancer) of DYRK1A.

CHAPTER 5: CONCLUSION

In summary, this study reports validation of the interaction between DYRK1A and seven proteins previously identified as DYRK1A candidate binding partners. Given lack of functional data about these proteins, we also generated tools and performed their initial functional characterization. We found that DYRK1A interacting proteins shown in this study also interacted with a previously reported DYRK1A-binding scaffold protein DCAF7. The N-terminal domain of DYRK1A was required for its interaction with DCAF7. Furthermore, the requirement of this region of DYRK1A for the binding to LZTS1, LZTS2 and FAM117B suggests that DCAF7 mediates the interaction between DYRK1A and these proteins. Further studies are needed to test this model. We observed that DYRK1A interacting proteins were localized in different cellular compartments and established that they have differential effects on cell morphology and proliferation. Our findings suggest that DYRK1A could play specific roles in different cellular compartments and that DYRK1A-interacting proteins could both contribute to its growth

suppressor function and antagonize it. Further mechanistic studies using our established cell-based model systems will help to understand the function and regulation of DYRK1A.

LIST OF REFERENCES

1. Alvarez, M. (2003). DYRK1A accumulates in splicing speckles through a novel targeting signal and induces speckle disassembly. *Journal of Cell Science*, 116(15), pp.3099-3107.
2. Alvarez, M., Altafaj, X., Aranda, S. and de la Luna, S. (2007). DYRK1A Autophosphorylation on Serine Residue 520 Modulates Its Kinase Activity via 14-3-3 Binding. *Molecular Biology of the Cell*, 18(4), pp.1167-1178.
3. Aranda, S., Laguna, A. and de la Luna, S. (2010). DYRK family of protein kinases: evolutionary relationships, biochemical properties, and functional roles. *The FASEB Journal*, 25(2), pp.449-462.
4. Baffa, R., Fassan, M., Sevignani, C., Vecchione, A., Ishii, H., Giarnieri, E., Iozzo, R., Gomella, L. and Croce, C. (2008). Fez1/Lzts1-deficient mice are more susceptible to N-butyl-N-(4-hydroxybutil) nitrosamine (BBN) carcinogenesis. Carcinogenesis, 29(4), pp.846-848.
5. Becker, W. and Joost, H. (1999). Structural and Functional Characteristics of Dyrk, a Novel Subfamily of Protein Kinases with Dual Specificity. *Prog Nucleic Acid Res Mol Biol*, 62, pp.1-17.

6. Becker, W., Weber, Y., Wetzel, K., Eirmbter, K., Tejedor, F. and Joost, H. (1998). Sequence Characteristics, Subcellular Localization, and Substrate Specificity of DYRK-related Kinases, a Novel Family of Dual Specificity Protein Kinases. Journal of Biological Chemistry, 273(40), pp.25893-25902.
7. Branchi, I., Bichler, Z. and Minghetti, L. (2004). Transgenic mouse in vivo library of human Down syndrome critical region 1, association between DYRK1A overexpression, brain development abnormalities, and cell cycle protein alteration. *J. Neuropathol. Exp. Neurol*, 63, pp.429-440.
8. Cabeza-Arvelaiz, Y., Thompson, T., Sepulveda, J. and Chinault, A. (2001). LAPSER1: a novel candidate tumor suppressor gene from 10q24.3. Oncogene, 20(46), pp.6707-6717.
9. Cam, H., Balciunaite, E., Blais, A., Spektor, A., Scarpulla, R., Young, R., Kluger, Y. and Dynlacht, B. (2004). A Common Set of Gene Regulatory Networks Links Metabolism and Growth Inhibition. Molecular Cell, 16(3), pp.399-411.
10. Cobrinik, D. (2005). Pocket proteins and cell cycle control. Oncogene, 24(17), pp.2796-2809.
11. Couzens, A., Knight, J., Kean, M., Teo, G., Weiss, A., Dunham, W., Lin, Z., Bagshaw, R., Sicheri, F., Pawson, T., Wrana, J., Choi, H. and Gingras, A. (2013). Protein Interaction Network of the Mammalian Hippo Pathway Reveals Mechanisms of Kinase-Phosphatase Interactions. Science Signaling, 6(302), pp.rs15-rs15.
12. Cui, Q., Tang, Z., Zhang, X., Zhao, H., Dong, Q., Xu, K. and Wang, E. (2013). Leucine Zipper Tumor Suppressor 2 Inhibits Cell Proliferation and Regulates Lef/Tcf-dependent Transcription through Akt/GSK3 Signaling Pathway in Lung Cancer. Journal of Histochemistry & Cytochemistry, 61(9), pp.659-670.

13. Dannenberg JH, te Riele HP. (2006). The retinoblastoma gene family in cell cycle regulation and suppression of tumorigenesis. Results Probl Cell Differ 42,pp.183–225.
14. Degoutin, J., Milton, C., Yu, E., Tipping, M., Bosveld, F., Yang, L., Bellaiche, Y., Veraksa, A. and Harvey, K. (2013). Riquiqui and Minibrain are regulators of the Hippo pathway downstream of Dachsous. Nat Cell Biol, 15(10), pp.1176-1185.
15. Di Vona, C., Bezdan, D., Islam, A., Salichs, E., López-Bigas, N., Ossowski, S. and de la Luna, S. (2015). Chromatin-wide Profiling of DYRK1A Reveals a Role as a Gene-Specific RNA Polymerase II CTD Kinase. Molecular Cell, 57(3), pp.506-520.
16. Dick, F. and Mymryk, J. (2011). Sweet DREAMs for Hippo. Genes & Development, 25(9), pp.889-894.
17. Ferrer, I., Barrachina, M., Puig, B., Martínez de Lagrán, M., Martí, E., Avila, J. and Dierssen, M. (2005). Constitutive Dyrk1A is abnormally expressed in Alzheimer disease, Down syndrome, Pick disease, and related transgenic models. *Neurobiology of Disease*, 20(2), pp.392-400.
18. Fotaki, V., Dierssen, M., Alcantara, S., Martinez, S., Marti, E., Casas, C., Visa, J., Soriano, E., Estivill, X. and Arbones, M. (2002). Dyrk1A Haploinsufficiency Affects Viability and Causes Developmental Delay and Abnormal Brain Morphology in Mice. *Molecular and Cellular Biology*, 22(18), pp.6636-6647.
19. Fukuda, M. and Nozawa, S. (1999). Trophinin, Tastin, and Bystin: A Complex Mediating Unique Attachment Between Trophoblastic and Endometrial Epithelial Cells at Their Respective Apical Cell Membranes. Seminars in Reproductive Medicine, 17(03), pp.229-234.

20. Guimera, J., Casas, C., Estivill, X. and Pritchard, M. (1999). HumanMinibrainHomologue (MNBH/DYRK1): Characterization, Alternative Splicing, Differential Tissue Expression, and Overexpression in Down Syndrome. *Genomics*, 57(3), pp.407-418.
21. Harvey, K., Zhang, X. and Thomas, D. (2013). The Hippo pathway and human cancer. Nat Rev Cancer, 13(4), pp.246-257.
22. Himpel, S., Panzer, P., Eirmbter, K., Czajkowska, H., Sayed, M., Packman, L., Blundell, T., Kentrup, H., Grötzinger, J., Joost, H. and Becker, W. (2001). Identification of the autophosphorylation sites and characterization of their effects in the protein kinase DYRK1A. *Biochem. J.*, 359(3), p.497.
23. Himpel, S., Panzer, P., Eirmbter, K., Czajkowska, H., Sayed, M., Packman, L., Blundell, T., Kentrup, H., Grötzinger, J., Joost, H. and Becker, W. (2001). Identification of the autophosphorylation sites and characterization of their effects in the protein kinase DYRK1A. *Biochem. J.*, 359(3), p.497.
24. Himpel, S., Tegge, W., Frank, R., Leder, S., Joost, H. and Becker, W. (2000). Specificity Determinants of Substrate Recognition by the Protein Kinase DYRK1A. *Journal of Biological Chemistry*, 275(4), pp.2431-2438.
25. Ishii, H., Baffa, R., Numata, S., Murakumo, Y., Rattan, S., Inoue, H., Mori, M., Fidanza, V., Alder, H. and Croce, C. (1999). The FEZ1 gene at chromosome 8p22 encodes a leucine-zipper protein, and its expression is altered in multiple human tumors. Proceedings of the National Academy of Sciences, 96(7), pp. 3928-3933.

26. Jin, J., Arias, E., Chen, J., Harper, J. and Walter, J. (2006). A Family of Diverse Cul4-Ddb1-Interacting Proteins Includes Cdt2, which Is Required for S Phase Destruction of the Replication Factor Cdt1. Molecular Cell, 23(5), pp.709-721.

27. Kaczmarski, W., Barua, M., Mazur-Kolecka, B., Frackowiak, J., Dowjat, W., Mehta, P., Bolton, D., Hwang, Y., Rabe, A., Albertini, G. and Wegiel, J. (2014). Intracellular distribution of differentially phosphorylated dual-specificity tyrosine phosphorylation-regulated kinase 1A (DYRK1A). Journal of Neuroscience Research, 92(2), pp.162-173.

28. Kinstrie, R., Lochhead, P., Sibbet, G., Morrice, N. and Cleghon, V. (2006). dDYRK2 and Minibrain interact with the chromatin remodelling factors SNR1 and TRX. *Biochem. J.*, 398(1), p.45.

29. Koreth, J. and van den Heuvel, S. (2005). Cell-cycle control in Caenorhabditis elegans: how the worm moves from G1 to S. *Oncogene*, 24(17), pp.2756-2764.

30. Lee, J. and Zhou, P. (2007). DCAFs, the Missing Link of the CUL4-DDB1 Ubiquitin Ligase. Molecular Cell, 26(6), pp.775-780.

31. Li, D. and Roberts, R. (2001). Human Genome and Diseases: WD-repeat proteins: structure characteristics, biological function, and their involvement in human diseases. Cellular and Molecular Life Sciences, 58(14), pp.2085-2097.

32. Li, K., Zhao, S., Karur, V. and Wojchowski, D. (2002). DYRK3 Activation, Engagement of Protein Kinase A/cAMP Response Element-binding Protein, and Modulation of Progenitor Cell Survival. *Journal of Biological Chemistry*, 277(49), pp.47052-47060.

33. Link, AJ., Washburn, MP. 2014. Analysis of protein composition using multidimensional chromatography and mass spectrometry. Curr Protoc Protein Sci. 78, pp.23.1.1-23.1.25.

34. Litovchick, L., Florens, L., Swanson, S., Washburn, M. and DeCaprio, J. (2011). DYRK1A protein kinase promotes quiescence and senescence through DREAM complex assembly. *Genes & Development*, 25(8), pp.801-813.

35. Litovchick, L., Sadasivam, S., Florens, L., Zhu, X., Swanson, S., Velmurugan, S., Chen, R., Washburn, M., Liu, X. and DeCaprio, J. (2007). Evolutionarily Conserved Multisubunit RBL2/p130 and E2F4 Protein Complex Represses Human Cell Cycle-Dependent Genes in Quiescence. Molecular Cell, 26(4), pp.539-551.

36. Liu, F., Li, B., Tung, E., Grundke-Iqbal, I., Iqbal, K. and Gong, C. (2007). Site-specific effects of tau phosphorylation on its microtubule assembly activity and self-aggregation. European Journal of Neuroscience, 26(12), pp.3429-3436.

37. Liu, F., Liang, Z., Wegiel, J., Hwang, Y., Iqbal, K., Grundke-Iqbal, I., Ramakrishna, N. and Gong, C. (2008). Overexpression of Dyrk1A contributes to neurofibrillary degeneration in Down syndrome. *The FASEB Journal*, 22(9), pp.3224-3233.

38. Lochhead, P., Sibbet, G., Kinstrie, R., Cleghon, T., Rylatt, M., Morrison, D. and Cleghon, V. (2003). dDYRK2: a novel dual-specificity tyrosine-phosphorylation-regulated kinase in Drosophila. *Biochem. J.*, 374(2), p.381.

39. Lochhead, P., Sibbet, G., Morrice, N. and Cleghon, V. (2005). Activation-Loop Autophosphorylation Is Mediated by a Novel Transitional Intermediate Form of DYRKs. Cell, 121(6), pp.925-936.

40. Lovat, F., Ishii, H., Schiappacassi, M., Fassan, M., Barbareschi, M., Galligioni, E., Vecchione, A. (2014). LZTS1 downregulation confers paclitaxel resistance and is associated with worse prognosis in breast cancer.*Oncotarget*, *5*(4), pp. 970–977.

41. Malumbres, M. and Barbacid, M. (2001). Milestones In Cell Division To Cycle Or Not To Cycle: A Critical Decision In Cancer. *Nat. Rev. Cancer.*, 1(3), pp.222-231.

42. Malumbres, M. and Barbacid, M. (2009). Cell cycle, CDKs and cancer: a changing paradigm. Nat Rev Cancer, 9(3), pp.153-166.

43. Massagué, J. (2004). G1 cell-cycle control and cancer. *Nature*, 432(7015), pp.298-306.

44. Miller, J., Yeh, N., Vidal, A. and Koff, A. (2007). Interweaving the Cell Cycle Machinery with Cell Differentiation. *Cell Cycle*, 6(23), pp.2932-2938.

45. Miyata, Y. and Nishida, E. (2011). DYRK1A binds to an evolutionarily conserved WD40-repeat protein WDR68 and induces its nuclear translocation. Biochimica et Biophysica Acta (BBA) - Molecular Cell Research, 1813(10), pp.1728-1739.

46. Moeller, R., Kübart, S., Hoeltzenbein, M., Heye, B., Vogel, I., Hansen, C., Menzel, C., Ullmann, R., Tommerup, N., Ropers, H., Tümer, Z. and Kalscheuer, V. (2008). Truncation of the Down Syndrome Candidate Gene DYRK1A in Two Unrelated Patients with Microcephaly. *The American Journal of Human Genetics*, 82(5), pp.1165-1170.

47. Morita, K., Celso, C., Spencer-Dene, B., Zouboulis, C. and Watt, F. (2006). HAN11 binds mDia1 and controls GLI1 transcriptional activity. Journal of Dermatological Science, 44(1), pp.11-20.

48. Nadano, D., Nakayama, J., Matsuzawa, S., Sato, T., matsuda, T. and Fukuda, M. (2002). Human tastin, a proline-rich cytoplasmic protein, associates with the microtubular cytoskeleton. Biochem. J., 364(3), p.669.

49. Nissen,R M., Amsterdam A., Hopkins N. (2006) *A zebrafish screen for craniofacial mutants identifies wdr68 as a highly conserved gene required for endothelin-1 expression* BMC Dev. Biol., 6, pp. 28–44.

50. Okui, M., Ide, T., Morita, K., Funakoshi, E., Ito, F., Ogita, K., Yoneda, Y., Kudoh, J. and Shimizu, N. (1999). High-Level Expression of the Mnb/Dyrk1A Gene in Brain and Heart during Rat Early Development. *Genomics*, 62(2), pp.165-171.

51. Park, J., Sung, J., Park, J., Song, W., Chang, S. and Chung, K. (2012). Dyrk1A negatively regulates the actin cytoskeleton through threonine phosphorylation of N-WASP. Journal of Cell Science, 125(1), pp.67-80.

52. Pellegrin, S. and Mellor, H. (2007). Actin stress fibres. Journal of Cell Science, 120(20), pp.3491-3499.

53. Poulsen, M., Lukas, C., Lukas, J., Bekker-Jensen, S. and Mailand, N. (2012). Human RNF169 is a negative regulator of the ubiquitin-dependent response to DNA double-strand breaks. The Journal of Cell Biology, 197(2), pp.189-199.

54. Proteome.org.au, (n.d.). [online] Available at: http://www.proteome.org.au/Images/UserUploadedImages/133/PULLdownA.jpg [Accessed 11 Apr. 2015].

55. Ritterhoff, S., Farah, C., Grabitzki, J., Lochnit, G., Skurat, A. and Schmitz, M. (2010). The WD40-repeat protein Han11 functions as a scaffold protein to control HIPK2 and MEKK1 kinase functions. The EMBO Journal, 29(22), pp.3750-3761.

56. Schirmer, E. (2009). MudPIT: A Powerful Proteomics Tool for Discovery. Discovery Medicine.

57. Schmit, F., Korenjak, M., Mannefeld, M., Schmitt, K., Franke, C., von Eyss, B., Gagrica, S., Hanel, F., Brehm, A. and Gaubatz, S. (2007). LINC, a Human Complex That is Related to pRB-Containing Complexes in Invertebrates Regulates the Expression of G 2 /M Genes. Cell Cycle, 6(15), pp.1903-1913.

58. Skurat, A. and Dietrich, A. (2003). Phosphorylation of Ser 640 in Muscle Glycogen Synthase by DYRK Family Protein Kinases. Journal of Biological Chemistry, 279(4), pp.2490-2498.

59. Smith EJ, Leone G, DeGregori J, Jakoi L, Nevins JR. (1996). The accumulation of an E2F-p130 transcriptional repressor distinguishes a G0 cell state from a G1 cell state. Mol Cell Biol 16,pp.6965–6976.

60. Smith, T., Gaitatzes, C., Saxena, K. and Neer, E. (1999). The WD repeat: a common architecture for diverse functions. Trends in Biochemical Sciences, 24(5), pp.181-185.

61. Song, M., Salmena, L., Carracedo, A., Egia, A., Lo-Coco, F., Teruya-Feldstein, J. and Pandolfi, P. (2008). The deubiquitinylation and localization of PTEN are regulated by a HAUSP–PML network. Nature, 455(7214), pp.813-817.

62. Soppa, U., Schumacher, J., Florencio Ortiz, V., Pasqualon, T., Tejedor, F. and Becker, W. (2014). The Down syndrome-related protein kinase DYRK1A phosphorylates p27 Kip1 and Cyclin D1 and induces cell cycle exit and neuronal differentiation. Cell Cycle, 13(13), pp.2084-2100.

63. Sudo, H. and Maru, Y. (2008). LAPSER1/LZTS2: a pluripotent tumor suppressor linked to the inhibition of katanin-mediated microtubule severing. Human Molecular Genetics, 17(16), pp.2524-2540.

64. Tejedor, F. and Hämmerle, B. (2010). MNB/DYRK1A as a multiple regulator of neuronal development. *FEBS Journal*, 278(2), pp.223-235.

65. Tejedor, F., Zhu, X., Kaltenbach, E., Ackermann, A., Baumann, A., Canal, I., Heisenberg, M., Fischbach, K. and Pongs, O. (1995). minibrain: A new protein kinase

family involved in postembryonic neurogenesis in Drosophila. *Neuron*, 14(2), pp.287-301.

66. Thyssen, G., Li, T., Lehmann, L., Zhuo, M., Sharma, M. and Sun, Z. (2006). LZTS2 Is a Novel -Catenin-Interacting Protein and Regulates the Nuclear Export of -Catenin. Molecular and Cellular Biology, 26(23), pp.8857-8867.
67. Trotman, L., Wang, X., Alimonti, A., Chen, Z., Teruya-Feldstein, J., Yang, H., Pavletich, N., Carver, B., Cordon-Cardo, C., Erdjument-Bromage, H., Tempst, P., Chi, S., Kim, H., Misteli, T., Jiang, X. and Pandolfi, P. (2007). Ubiquitination Regulates PTEN Nuclear Import and Tumor Suppression. Cell, 128(1), pp.141-156.
68. Tschop, K., Conery, A., Litovchick, L., DeCaprio, J., Settleman, J., Harlow, E. and Dyson, N. (2011). A kinase shRNA screen links LATS2 and the pRB tumor suppressor. Genes & Development, 25(8), pp.814-830.
69. Van der Horst, A., de Vries-Smits, A., Brenkman, A., van Triest, M., van den Broek, N., Colland, F., Maurice, M. and Burgering, B. (2006). FOXO4 transcriptional activity is regulated by monoubiquitination and USP7/HAUSP. Nat Cell Biol, 8(10), pp.1064-1073.
70. Varjosalo, M., Keskitalo, S., Van Drogen, A., Nurkkala, H., Vichalkovski, A., Aebersold, R. and Gstaiger, M. (2013). The Protein Interaction Landscape of the Human CMGC Kinase Group. Cell Reports, 3(4), pp.1306-1320.
71. Vecchione, A., Baldassarre, G., Ishii, H., Nicoloso, M., Belletti, B., Petrocca, F., Zanesi, N., Fong, L., Battista, S., Guarnieri, D., Baffa, R., Alder, H., Farber, J., Donovan, P. and Croce, C. (2007). Fez1/Lzts1 Absence Impairs Cdk1/Cdc25C Interaction during Mitosis and Predisposes Mice to Cancer Development. Cancer Cell, 11(3), pp.275-289.

72. Vidwans, S. and Su, T. (2001). Cycling through development in Drosophila and other metazoa. *Nature Cell Biology*, 3(1), pp.E35-E39.

73. Vogelstein, B., Lane, D.,Levine, AJ. (2000) Surfing the p53 network Nature, 408, pp. 307–310.

74. Wegiel, J., Dowjat, K., Kaczmarski, W., Kuchna, I., Nowicki, K., Frackowiak, J., Mazur Kolecka, B., Wegiel, J., Silverman, W., Reisberg, B., deLeon, M., Wisniewski, T., Gong, C., Liu, F., Adayev, T., Chen-Hwang, M. and Hwang, Y. (2008). The role of overexpressed DYRK1A protein in the early onset of neurofibrillary degeneration in Down syndrome. *Acta Neuropathologica*, 116(4), pp.391-407.

75. Wegiel, J., Gong, C. and Hwang, Y. (2011). The role of DYRK1A in neurodegenerative diseases. *FEBS Journal*, 278(2), pp.236-245.

76. Yabut, O., Domogauer, J. and D'Arcangelo, G. (2010). Dyrk1A Overexpression Inhibits Proliferation and Induces Premature Neuronal Differentiation of Neural Progenitor Cells. *Journal of Neuroscience*, 30(11), pp.4004-4014.

77. Yang, S., Liu, X., Yin, Y., Fukuda, M. and Zhou, J. (2008). Tastin is required for bipolar spindle assembly and centrosome integrity during mitosis. The FASEB Journal, 22(6), pp.1960-1972.

ERRATUM

This page contains an erratum for errors identified as of August 2016 in the master's thesis of Varsha Ananthapadmanabhan titled 'Understanding the function of DYRK1A through characterization of its interacting proteins' published in VCU scholars compass in May 2015.

1) An error has been identified in panel A of Figure 19 in the thesis. The blot for the input panel for GFP was incorrectly placed. The blot for Vinculin and HA were not aligned properly. Below is the correct version of the figure.

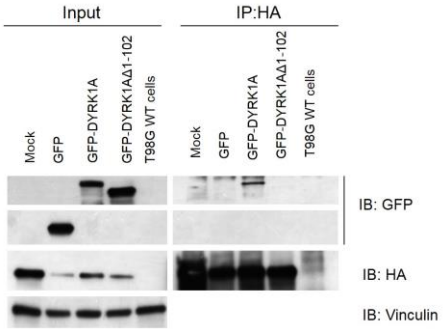

2) The constructs used for the protein FAM117B in the thesis was found to not encode the full length of the protein in subsequent studies. The construct encoding the protein has a deletion of the first 731 bases of the coding DNA resulting in a protein that had a deletion of the first 244 amino acids resulting in a shorter protein having amino acids 245- 589 of the full length protein.